

CosmicMan: A Text-to-Image Foundation Model for Humans

Shikai Li*, Jianglin Fu*, Kaiyuan Liu*, Wentao Wang*, Kwan-Yee Lin†, Wayne Wu†
Shanghai AI Laboratory

{lishikai, fujianglin, wangwentao}@pjlab.org.cn

1154864382@mail.dlut.edu.cn linjunyi9335@gmail.com wuwenyan0503@gmail.com

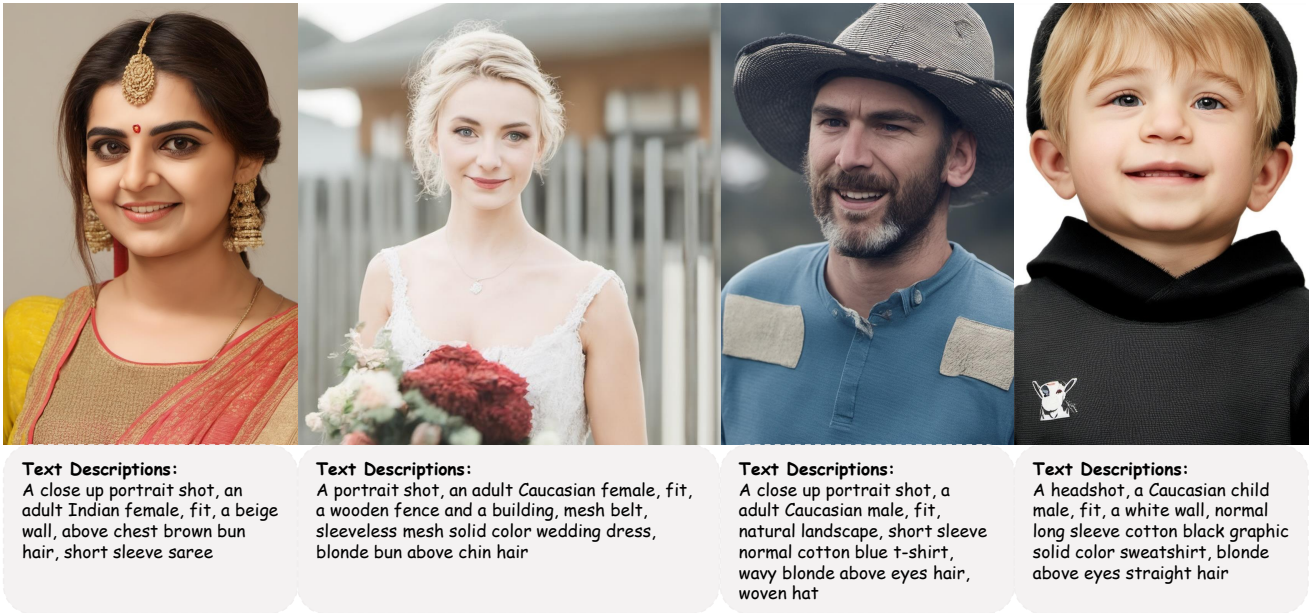


Figure 1. **CosmicMan**. High-fidelity images generated by our proposed human-specialized text-to-image foundation model CosmicMan. The results are with meticulous appearance, reasonable structure, and precise text-image alignment with detailed dense descriptions. More results are presented in the project page: <https://cosmicman-cvpr2024.github.io/>.

Abstract

We present **CosmicMan**, a text-to-image foundation model specialized for generating high-fidelity human images. Unlike current general-purpose foundation models that are stuck in the dilemma of inferior quality and text-image misalignment for humans, **CosmicMan** enables generating photo-realistic human images with meticulous appearance, reasonable structure, and precise text-image alignment with detailed dense descriptions.

At the heart of **CosmicMan**'s success are the new reflections and perspectives on data and models: (1) We found that data quality and a scalable data production flow are essential for the final results from trained models. Hence, we

propose a new data production paradigm, **Annotate Anyone**, which serves as a perpetual data flywheel to produce high-quality data with accurate yet cost-effective annotations over time. Based on this, we constructed a large-scale dataset, **CosmicMan-HQ 1.0**, with 6 Million high-quality real-world human images in a mean resolution of 1488×1255 , and attached with precise text annotations deriving from 115 Million attributes in diverse granularities. (2) We argue that a text-to-image foundation model specialized for humans must be pragmatic – easy to integrate into downstream tasks while effective in producing high-quality human images. Hence, we propose to model the relationship between dense text descriptions and image pixels in a decomposed manner, and present **Decomposed-Attention-Refocusing (Daring)** training framework. It seamlessly decomposes the cross-attention features in existing text-to-

*Joint first authors.

†Equal advising.

image diffusion model, and enforces attention refocusing without adding extra modules. Through *Daring*, we show that explicitly discretizing continuous text space into several basic groups that align with human body structure is the key to tackling the misalignment problem in a breeze.

1. Introduction

Text-to-image foundation models, *e.g.*, Stable Diffusion (SD) [51], Imagen [53], and DALLE [48], have made groundbreaking contributions in the realm of Computer Vision and Graphics. These models, fueled by expansive image-text datasets [3, 55] and advanced generative algorithms [13, 22, 60], possess the capability to create images of remarkable quality and details. These models, underpinned by robust prior knowledge, have significantly enhanced a wide array of downstream tasks. Notable examples include DreamBooth [52] and ControlNet [67] in 2D image generation, alongside DreamFusion [46] and Zero-1-to-3 [36] in 3D object creation. Despite these advances, a critical gap remains within the sphere of *human-centric* content generation – the absence of a specialized text-to-image foundation model that serves as a cornerstone for tasks on human subjects.

In prior research, tasks related to human-centric content generation, like 2D human generation/editing [16, 26, 33] and 3D human generation/reconstruction [18, 54, 65, 66], have typically progressed in isolation, each relying on its in-domain data. These methods, however, faced a key limitation: the datasets used were often narrow in diversity [7], exhibited biased distributions [16], or lacked quality [29]. Achieving *generalization* across a broad range of identities, appearances, and geometries in real-world applications has been challenging within this framework. Nevertheless, the emergence of text-to-image foundation models, which have excelled in the general-purpose arena, offers a promising new direction to revolutionize human-centric content generation with enhanced generalization capabilities.

The pivotal question then arises: *How to obtain a text-to-image foundation model for humans?* By analyzing the essential demands of a human-specialized foundation model, we identify three critical elements necessary for such a model: 1) **High-Quality Data**. To train a foundation model that will be used in downstream tasks to generate high-quality content, the raw data quality is critical. The raw data quality encompasses not only the volume but also the image quality and diversity, as well as the precision, granularity, and comprehensiveness of annotations. While large-scale datasets featuring text-image pairs (*e.g.*, LAION-5B [55], and COYO-700M [3]) have advanced general-purpose foundation models, they often deviate from accurately representing real-world human distributions, suffering from jagged image quality and a mass of

annotation noise. 2) **Scalable Data Production**. A foundation model that generalizes effectively must evolve in sync with the growth of real-world data. Given the vast amount of training data that is requisite and the rapid pace at which it expands in human contexts, developing a scalable data production process is imperative – being updated over time and cost-effective. Traditional methods often incur high costs due to manual annotation [1, 35, 44, 57], or suffer from accuracy issues when using automated labeling [56]. Moreover, the reliance on static datasets limits their ability to adjust according to dynamic real-world data distributions. 3) **Pragmatic Model**. A foundation model designed for humans should be straightforward to integrate into downstream tasks, requiring minimal customization of its architecture. In addition, given the complexity of human anatomy, the ability of a model to generate high-quality outputs is also essential – the outputs should guarantee realistic structures and precise text-image alignment, especially capturing detailed dense concepts attached to humans. Existing models, whether closed-source like MidJourney [39], DALLE [48], or those struggling with high-fidelity human generation such as SD [51] and SDXL [45], highlight the need for a versatile, high-quality model tailored for human-centric applications.

We present **CosmicMan** – a holistic solution of text-to-image foundation model for humans. We first introduce a new data production paradigm *Annotate Anyone* by human-AI cooperation, which can produce flowing, high-quality yet cost-effective data continuously. *Annotate Anyone* consists of two main stages: *Flowing Data Sourcing* to get a flowing data pool with irrigated high-quality human images from academic datasets and Internet, and *Human-in-the-loop Data Annotation* to iteratively refine the labeling quality of the data in the pool at a fairly low cost. Then, a data flywheel is constructed to produce vast amounts of data in a dynamic, up-to-date, and economical manner, which is well-adaptive in the age of large-scale foundation models.

By running *Annotate Anyone*, we constructed a large-scale, high-quality dataset, *CosmicMan-HQ 1.0*, which currently included 6 million human images with a mean resolution of 1488×1255 . It includes rich annotations with high precision – 115 million attributes, texts, bounding boxes, keypoints, human parsings, and rich meta information. Empowered by *Annotate Anyone*, *CosmicMan-HQ* continues to grow rapidly. Future versions of *CosmicMan-HQ* will support the perpetual update of foundation models with growing real-world data, facilitating long-term research in human-centric generation.

Finally, based on *CosmicMan-HQ*, we provide a human-specialized foundation model to support the human-centric content generation tasks. To ensure the easy of use of the proposed model, we construct our model by tailoring SD with minimum modification. Concretely, we intro-

duce *Decomposed-Attention-Refocusing (Daring)*, a training framework that is rooted in SD without adding extra modules. In virtue of the nature of the proposed dataset, the key insight of the framework is explicitly discretizing dense descriptions into a fixed number of groups related to human body structure. Based on this, we could decompose the cross-attention feature maps according to the groups and enforce the network learning attention refocusing at the group level. This target could be achieved by adding a new loss supervised on cross-attention maps, called *HOLA* (short for *Human Body and Outfit Guided Loss for Alignment*).

In experiments, we demonstrate superior image quality and text-image alignment by comparing our models to state-of-the-art foundation models. Then, we conduct extensive ablation studies to show the effectiveness of our designs in data production and model training. Finally, we show the practicality and potential of our human-specialized foundation model with applications in 2D and 3D generation.

2. Related Work

2.1. Text-to-Image Foundation Models

Advancements in data volume and model design have led text-to-image foundation models to produce high-fidelity images that follow the text instructions. DALLE [48], which pioneered zero-shot text-to-image generation, autoregressively modeling text and image tokens in a unified data stream. Its successors [2, 49] enhance performance through model design and improved captions. Imagen [53] utilizes a larger text encoder with better photo realism. Open-source models like DeepFloyd-IF [11], PixelArt- α [6], and particularly SD [51], along with SDXL [45], have energized the community, accelerating various applications in downstream tasks. In 2D content generation, innovations like ControlNet [67] and T2I-Adapter [41] have emerged, and in 3D, models like Zero-1-to-3 [36] and DreamFusion [46] leverage SD to create high-quality 3D objects. However, these foundation models are geared towards the general-purpose domain, which falls short in generating humans due to their tendency to overlook the nuances and complexities of human anatomy and attire. There is still a gap for a human-specialized text-to-image foundation model to boost downstream human content generation.

2.2. Text-Driven Human Image Generation

Previous research [26, 33, 40, 42] primarily focused on fashion-domain data and has achieved high-fidelity human generation and editing with control over text. For instance, Text2Human [26] employs a two-stage framework using VQ-VAE [60] to transfer human pose into human parsing with cloth shape and generates human images with texture description. FashionTex [33] offers text and texture-based control for virtual try-on by leveraging the pretrained

generative models [16]. However, the extremely biased and insufficient training data, hinder the diversity of generated images from these methods. Meanwhile, some approaches [29, 67] leverage text-to-image foundation models [51] to create more diverse human images with additional conditions (*e.g.*, skeletons and normal maps). HumanSD [29] introduces a skeleton-guided diffusion model trained on a diverse dataset that enhances the accuracy of pose control. However, these methods are used for controllable human image generation. In contrast, CosmicMan stands out as a foundation model by producing high-quality and diverse human images without relying on spatial conditions in the inference phase.

2.3. Text-Image Alignment for Dense Concepts

Early text-to-image models, often trained on short text captions, struggle to encapsulate dense concepts present in longer descriptions. The dense concepts, as discussed in many text-to-image benchmarks [17, 23], include multiple objects, attributes, and spatial relationships that describe the image from different granularities and perspectives. The challenge lies in generating each element and accurately depicting their interrelations within long descriptions. Recently, the training-free methods [5, 14, 19, 32, 50, 62, 69] found that the cross-attention mechanism plays a pivotal role in text-to-image alignment. Prompt-to-Prompt [19] first reveals that the cross-attention map governs the semantics of the output. Subsequent methods [5, 32, 62, 69] are proposed to employ the gradients of the well-designed loss to update the latent feature along the diffusion process. Additionally, FastComposer [64] applies the supervision of cross-attention maps during training. However, intuitively applying this to human images becomes more complex, as dense captions for humans often cluster in a small image region, as shown in Fig. 3. Thus, we propose a training framework that utilizes human-specific prior on arrangement relationships to supervise the cross-attention maps with decomposed text-human image data, which further improves the text-image alignment on dense concepts.

3. Annotate Anyone – A Data Flywheel

To enable the learning of the human-specialized foundation model, we propose a human-AI cooperation paradigm for data production named **Annotate Anyone**. It combines the strengths of AI and human expertise to build a continuously expandable dataset CosmicMan-HQ with rich annotations. In this section, we will first introduce Annotate Anyone by comparing to previous data production paradigms (Sec. 3.1). Then, we will elaborate on the procedures of Annotate Anyone in data sourcing and annotation (Sec. 3.2). Finally, we will analyze the statistics of CosmicMan-HQ 1.0 dataset produced by Annotate Anyone, and show its superiority to existing datasets (Sec. 3.3).

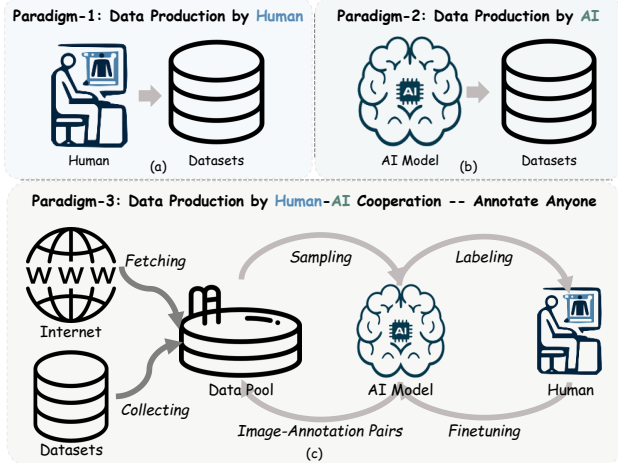


Figure 2. **Data Production Paradigm.** (a) Data production by humans and (b) data production by AI. (c) Our proposed new data production paradigm by Human-AI cooperation, named Annotate Anyone. It serves as a *data flywheel* to produce dynamic up-to-date high-quality data at a low cost.

3.1. Data Production by Human-AI Cooperation

To construct large-scale image datasets with labels, there are mainly two paradigms – by humans or by AI. Data production by humans (as depicted in Fig. 2 (a)) needs human annotators to manually label images one by one [12, 35, 70], which suffers from its high cost and thus is hard to scale up to support the recent development of large foundation models. On the other hand, data production by AI (as depicted in Fig. 2 (b)) uses off-the-shelf models to get labels for free [2, 6]. Although this paradigm dramatically reduces costs and is easy to scale up, it is notorious for its noisy, jagged, and coarse labeling results. Moreover, both of these paradigms rely on fixed datasets for labeling, which results in limited diversity and severe bias versus real-world data. To train a large foundation model, a huge quantity of data, high-precise and fine-grained labeling, and real-world distribution are all indispensable. Thus, these paradigms are especially knotty to adapt to the human domain.

To this end, we propose a new data production paradigm by *human-AI cooperation* named Annotate Anyone (as shown in Fig. 2 (c)). Compared to data production by humans and AI, Annotate Anyone pivots on two characteristics: 1) flowing data, and 2) human-in-the-loop annotation. Flowing data is sourced from two origins: existing published datasets and the Internet. By collecting data from existing published datasets, such as SHHQ [16] and LAION-5B [55], we can upcycle them to match the qualifications of a high-quality human dataset. By fetching data from the Internet, we can obtain the massive data produced by human beings every second. Our data sourcing system is

always on call to run when the data quantity triggers the lower-bound threshold. Thus, our data pool is continuously *flowing and refreshed*, which distinguishes it from previous paradigms. Human-in-the-loop annotation coordinates three entities: data pool, AI, and human annotators, to work in a circle. By labeling a small quantity of data with the greatest necessity, human annotators and AI models cooperate to iteratively improve the quality of data annotation. Consequently, data in the pool will have progressively better annotation quality at a minimal cost.

With Annotate Anyone, we construct a **data flywheel** to enable a dynamic up-to-date production of high-quality data. Consequently, just by running the Annotate Anyone workflow, we can construct a large-scale human dataset with continuously accumulated data with great ease.

3.2. Procedure of Annotate Anyone

The procedure of Annotate Anyone consists of two main parts: 1) flowing data sourcing to obtain and filter high-quality data from both academic datasets and the Internet continually, and 2) human-in-the-loop data annotation to get precise yet cost-effective labels covering detailed dense concepts and ensuring high-quality annotations.

3.2.1 Flowing Data Sourcing

We first source images from various origins to ensure massive quantity and catch the real-world distribution. Then, we design a data filter to eliminate unbecoming images for human content generation tasks.

Data Origins. We start with three *academic* datasets to recycle existing data resources: LAION-5B [55], SHHQ [16], and DeepFashion [37]. LAION-5B is a renowned collection of massive images shared online, while the other two datasets are smaller in scale and diversity but meticulously curated to ensure high quality. Then, we initiate 128 parallel processes in 32 CPU servers, monitoring a wide spectrum of APIs on the Internet, including Flickr [15], Unsplash [59], Pixabay [43], *etc.* These APIs give access to a vast collection of growing and diverse images, rendering a real-world distribution.

Data Filtering. The current data pool exhibits a broad distribution, but high-resolution human images are not the primary constituent. We use a set of data filtering strategies to distill a high-quality human-centric subset, including fake-people detection, image quality assessment, and so on. To remove fake-people images (*e.g.*, cartoon characters, mannequin models, and generated images), we fine-tuned EVA-CLIP [58] with Human-Art [28] and sets of fake images. The fine-tuned model with 91% accuracy is used to detect images containing fake people. Next, image quality assessment metrics (LIQE [68], IFQA [27], and HPSv2 [63]) are applied, estimating the image quality on both face and



Figure 3. **Parsing Examples from CosmicMan-HQ.** The parsing results of sampled image in our dataset, along with detailed labels for each part. Text descriptions are obtained from labels.

global levels, to streamline the data pool further. Further, we utilize YOLOv7 [61] to filter out images without humans or those containing more than one individual. Images where the largest detected face is smaller than 224×224 or where the image is smaller than 640×1280 are removed as well. See more details in the supplementary material.

3.2.2 Human-in-the-loop Data Annotation

Having a data pool with diverse and high-quality human images, the next step is to possess precise, fine-grained yet cost-effective annotations for the images. We propose a human-in-the-loop data annotation workflow to iteratively refine the labeling quality of the data in the pool. Below, we first introduce the annotation iteration and then discuss the label protocol we use to describe humans in a detailed way. **Annotation Iteration.** As shown in Fig. 2 (c), the iterations start from sampling an image set I_i from the data pool and end up with putting all image-annotation pairs (I, A) back to the data pool. We set an evaluation set I_e with ground truth. In each iteration, I_e is used to determine the categories that need to be labeled by human annotators, and I_i will be partially labeled with the selected categories. Then, I_i is used to finetune the AI model. The finetuned AI model is evaluated on I_e to determine whether to continue or stop the iterations. Finally, a well-finetuned AI model is used

to get image-annotation pair (I, A) for all data in the pool. Specifically, inspired by methods [2, 6] that use the Vision-Language Model (VLM) to perform image captioning tasks, we leverage a pretrained InstructBLIP [9] as our AI model in the iteration. Please refer to the supplementary for the pseudo-code of the annotation iteration.

The pivotal mechanism to implement the high-precise yet low-cost annotation is the trigger of human annotation. During the initial iteration, the annotation team labels all categories based on 70 questions. We observed that the accuracy of the predicted labels follows a real-world distribution, exhibiting a long-tail distribution. For the head categories, such as age and gender, the pretrained AI model already proficient in the prediction. Thus, in subsequent iterations, human annotators focus on tail categories, and categories with an accuracy above 85% will no longer be manually labeled. Our iterative process significantly improved the VLM model’s overall accuracy by at least 30% compared to the pretrained model. Moreover, the progressive reduction of labeled annotations during the iterations resulted in only 1% compared to full manual labeling. Please refer to the supplementary materials for experimental details.

Label Protocol. To systematically describe a human image comprehensively, we design a label protocol that leverages the human parsing model SCHP [31] to break down an image into 18 fine parts, including background, face, upper clothing, and *etc.* Each part has an average of 3 to 8 associated questions, resulting in a total of 70 questions that correspond to 70 categories. For example, “top-sleeve length” is one of the categories. The answers under each category form the detailed attributes in our dataset. For instance, the attributes associated with “top - sleeve length” include “long sleeve, mid-sleeve, sleeveless”, and so on. As shown in Fig. 3, for every single clothing item, once we confirm the existence of a particular garment, we proceed to further inquire about deeper detailed questions, such as color, pattern, and material. Questions related to global attributes are also asked. By employing this label protocol, we obtain a rich set of attributes regarding the human image with each label corresponding to a specific spatial position. Please refer to supplementary materials to see our final labeling results with the comparison to others.

3.3. CosmicMan-HQ 1.0 Dataset

By running Annotate Anyone, so far, the first version of the produced dataset CosmicMan-HQ 1.0 consists of 6M high-resolution, single-person images, along with corresponding rich annotations. Here we compare our dataset with representative human-centric datasets in terms of data quantity, imaging quality, and annotations.

As depicted in Tab. 1, our dataset is the largest crafted human-centric dataset, six times larger than LAION-Human [29]. The mean resolution is 1488×1255 , sur-

Table 1. **Dataset Comparison.** The statistical comparison between publicly available human-related datasets and CosmicMan-HQ 1.0. “Common Scale” refers to the dataset that includes images captured at common scales, such as full-body shots, portrait photos, and half-body shots. “HP” and “Aes” refer to Human Parsing maps and Aesthetic scores.

	Data Quantity			Imaging Quality		Annotation						Domain	
	Total Image #	Mean Resolution	Common Scale	Global↑	Face↑	Cat #	Attr #	Text	Bbox	Kpts	HP		Aes
Human-Art [28]	50K	1115 × 1287	✓	3.42	2.87	-	-	✓	✓	✓	✗	✗	Real world & AI Fashion
DF-MM [26]	44K	750 × 1101	✗	4.64	3.38	18	587K	✓	✓	✗	✓	✗	
LAION-Human [29]	1M	688 × 650	✓	4.20	2.66	-	-	✓	✗	✗	✗	✓	Real world Fashion
SHHQ 1.0 [16]	40K	1024 × 512	✗	4.23	2.13	-	-	✗	✗	✓	✓	✗	
CosmicMan-HQ 1.0	6M	1488 × 1255	✓	4.37	3.37	70	115M	✓	✓	✓	✓	✓	Real world

passing previous human-only datasets like DF-MM [26] and SHHQ [16] by a large margin. Our dataset possesses a diverse collection of human images, including full-body shots, headshots, half-body shots, and so on. In terms of image quality at both overall and face level, our dataset ranks second only to the fashion-focused DF-MM dataset, which predominantly contains professional studio images but with less diversity and a data amount. As for annotation, only DF-MM and ours provide manually labeled categories, but the former dataset is much smaller in data volume and category numbers. CosmicMan-HQ 1.0 provides 70 categories and around 115M detailed attributes as detailed in the Label Protocol part of Sec. 3.2.2.

Highlighting our dataset’s uniqueness, CosmicMan-HQ 1.0 distinguishes itself by providing an unparalleled wealth of diverse annotations, including 115M attributes, texts, bounding boxes, keypoints, human parsings, and rich meta information (web alternative texts, aesthetic scores, watermark scores, face/global quality scores, and camera EXIF parameters).

4. Daring - The Training Framework

We propose **Daring (Decomposed-Attention-Refocusing)**, a training framework rooted in original Stable Diffusion (SD) with minimal modification. The framework is illustrated in Fig. 4. It enjoys three properties at the same time – friendly to computational costs, compatible with downstream tasks supported by SD, and robust in producing high-quality human images that align well with dense concepts. These come from two parts’ design – data discretion for decomposing text-human image data (Sec. 4.2), and a new loss aiming to improve the alignment with respect to the scale of the human body and outfits (Sec. 4.3).

4.1. Preliminaries

We employ SD as the backbone model for its efficiency and widespread application in various downstream tasks. SD incorporates a variational autoencoder \mathcal{E} to encode images x as latent variables z in a compact latent space, and applies diffusion schema in the latent space, thereby facili-

tating the diffusion process and reducing the computational cost. The denoising network is optimized by minimizing the L_2 error between predicted noise ϵ_θ and ground-truth noise $\epsilon \sim \mathcal{N}(\mathbf{0}, \mathbf{I})$:

$$\mathcal{L}_{noise} = \mathbb{E}_{z \sim \mathcal{E}(x), c, \epsilon, t} [\|\epsilon - \epsilon_\theta(z_t, t, c)\|_2^2], \quad (1)$$

where z_t is the latent at time-step t , and c is the condition information that can be instantiated by text input.

The cross-attention layers are the hinge for textual information to play a role in influencing the updating of intermediate features. Specifically, a text prompt \mathcal{P} is first transformed into a text embedding c via a CLIP text encoder. The latent z_t and text embedding are projected to form a query Q and keys K . The cross-attention maps are computed to flatten textual information into spatial features:

$$M = \text{Softmax}\left(\frac{QK^T}{\sqrt{d}}\right) \quad (2)$$

where d is the dimension of Q and K embeddings. The design works well when the text descriptions are short sparse captions. However, it can not handle text information with dense concepts, due to the lack of effective guidance to learn distinctive and precisely located features.

4.2. Data Discretization for Humans

We argue that there is no necessity to optimize the latent code guided by cross-attention maps during inference or harm the original architecture design of SD with sophisticated modules, *as long as keys K are decomposable and finite at the first place*. This is doable and simple to achieve. Because for the human generation scenario, textual descriptions about a person always revolve around body structure and attachments. As humans are structured in nature, textual descriptions could be explicitly classified into fixed groups that correspond to body regions, no matter how many concepts are described.

Thus, rather than directly utilizing nature language description, we propose a discretized textual prototype as illustrated in Fig. 4 for the network to enable precise communication between tokens. The prototype defines the conven-

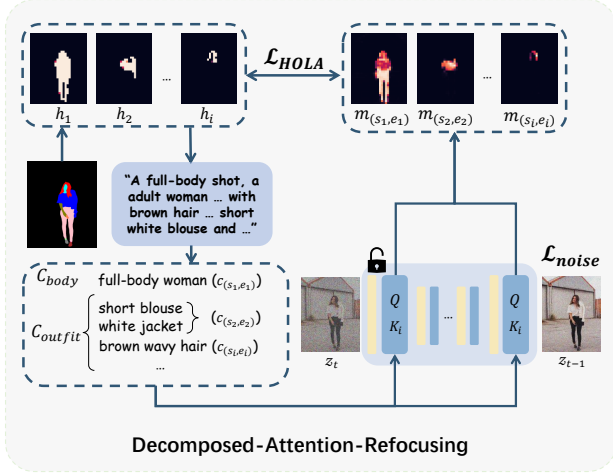


Figure 4. **Daring Training Framework.** It includes two parts: (1) data discretion for decomposing text-human data into fixed groups that obey human structure; (2) a new loss – HOLA, to enforce the cross-attention features actively response in proper spatial region with respect to the scale of body structure and outfit arrangement.

tion of classifying and arranging the concepts of text captions to a finite set, where all captions can be represented as $C = \{C_{body}, C_{outfit}\}$. The subset C_{body} is for overall appearance, and the subset C_{outfit} is for fine-grained attributes of outfits.

Concretely, as shown in Fig. 4, given a human data sample x in CosmicMan-HQ, we first reorganize human parsing maps into the semantic map sets $H = \{h_i\}_{i=1}^N$, where N is the number of semantic masks and h_1 is the aggregation of all human parsing maps to differentiate human foreground with background. These masks are categorized into two levels – h_1 lies in *human-body-level* and the others belong to *outfit-level*. Then, we split the text captions with respect to H . Specifically, $C_{body} = c_{(s_1, e_1)}$ and $C_{outfit} = \{c_{(s_2, e_2)}, \dots, c_{(s_N, e_N)}, c_{other}\}$. $c_{(s_n, e_n)}$ denotes the n^{th} sub-caption group related to the semantic map h_n , and s_n, e_n are the start and end indices of the concepts in the caption respectively. We gather the caption phrases without corresponding semantic masks as c_{other} , such as the caption for background. Note that, as our dataset naturally constructs annotation labels in a hierarchical manner, we can easily associate textual concepts with the semantic maps. For example, given a semantic map h_2 that represents the top clothing mask, we retrieve all the labels related to the top clothing and group them as a sub-caption c_2 .

4.3. Decomposing and Refocusing Features

During training diffusion models, the denoising loss \mathcal{L}_{noise} can ensure the content generative capability of the model, but it lacks explicit alignment constraints between the caption and image pixels, especially when encountering de-

scriptions with dense concepts that cover very high information density. Thus, on the shoulders of discrete human data mentioned in Sec. 4.2, we propose a new loss – HOLA (short for **H**uman **B**ody and **O**utfit **G**uided **L**oss for **A**lignment) to seamlessly decompose the cross-attention features in SD model and enforce attention refocusing without adding extra modules.

Concretely, given the caption C and latent z_t , the cross-attention maps M can be decomposed as $M = (m_{(s_1, e_1)}, m_{(s_2, e_2)}, \dots, m_{(s_N, e_N)}, m_{other})$. Each M_i is calculated through Eq. 2, with turning K to K_i (the projected embeddings of sub-caption $c_{(s_i, e_i)}$). We then incorporate HOLA alongside the original loss in SD to explicitly guide the cross-attention maps to have high responses only in specific regions. The HOLA is defined as follows:

$$\mathcal{L}_{HOLA} = \frac{1}{N} \sum_{i=1}^N \left(\sum_{j=s_i}^{e_i} \|m_j - h_i\|_2^2 + \left\| \frac{1}{e_i - s_i} \sum_{j=s_i}^{e_i} (m_j) - h_i \right\|_2^2 \right) \quad (3)$$

Specifically, the first term of HOLA works under the guidance of human body structure – it pushes the high response region of each concept feature to be as close as possible to the corresponding semantic region. However, since certain outfit-related concepts may only occupy a specific proportion within a semantic region, it is unnecessary to enforce their features to align with the whole semantic region. Also, concepts within the same group should be arranged harmoniously. Thus, we use the second term of HOLA to satisfy the situation. This term requires the average attention maps within one group to be close to their semantic map. It helps reduce ambiguities in outfit-level descriptions. The overall loss function is as follows:

$$\mathcal{L} = \alpha \mathcal{L}_{noise} + \beta \mathcal{L}_{HOLA} \quad (4)$$

where α and β are hyper-parameters to balance the contribution of each loss.

5. Experiments

In this section, we compare our method with SOTA text-to-image (T2I) methods on human-centric generation tasks. Sec. 5.1 shows experiment settings including implementation details and evaluation metrics. Sec. 5.2 validates our method outperforms state-of-the-art T2I methods from quantitative and human preference evaluation. Then, we provide an ablation study to evaluate the effectiveness of the design in training data and training strategy in Sec. 5.3. Finally, we show the practicality and potential of CosmicMan as a foundation model in Sec. 5.4, by the application in two representative tasks in 2D and 3D respectively – 2D human image editing and 3D human reconstruction.

Table 2. **Quantitative Comparison to SOTA Text-to-Image Models.** The best and second-best results are marked with **Red** and **Green**.

Methods	FID↓	HPSv2↑	CLIP↑	Acc _{obj} ↑	Acc _{tex} ↑	Acc _{shape} ↑	Acc _{all} ↑
SD 1.5 [51]	48.09	0.2659	30.43	87.3	77.4	59.3	74.6
SD 2.0 [51]	51.61	0.2588	26.27	82.8	74.7	58.7	72.0
SDXL [45]	48.61	0.2647	30.78	88.5	82.5	63.2	78.1
DeepFloyd-IF [11]	44.62	0.2603	29.33	87.9	84.4	62.0	78.1
DALLE-2 [49]	49.60	0.2630	29.86	83.3	79.3	55.3	72.6
DALLE-3 [2]	66.36	0.2673	28.86	86.2	87.1	60.1	77.8
MidJourney [39]	53.89	0.2688	28.89	85.2	79.5	59.4	74.7
CosmicMan-SD	36.78	0.2690	28.47	91.7	85.7	66.1	81.2
CosmicMan-SDXL	35.42	0.2698	27.31	92.7	88.3	69.7	83.6

5.1. Experimental Settings

Implementation Details. Our foundation models are based on Stable Diffusion (SD-1.5 [51] and SDXL [45]). We finetune the whole UNet from the pretrained model of Stable Diffusion combined with Daring framework on CosmicMan-HQ 1.0 dataset. We use AdamW [38] as the optimized method in 1e-5 learning rate and 1e-2 weight decay. Our model is trained on 32 80G NVIDIA A100 GPUs in a batch size of 64 for about one week. Please refer to the supplementary material for more details.

Evaluation Metrics. We evaluate results from three perspectives: 1) Image Quality: Frechet Inception Distance (FID) [21] and Human Preference Score v2 (HPSv2) [63] are used to reflect diversity and authenticity. 2) Text-Image Alignment: CLIPScore [20] provides a holistic measure of image-text alignment. However, it struggles to capture detailed image-text relationships, especially in fine-grained texture, shape, and object descriptions, which also be discussed in [8, 17, 23]. Our proposed semantic accuracy metric, inspired by DSG [8], enhances fine-grained text-image alignment, focusing on object (Acc_{obj}), texture (Acc_{tex}), shape (Acc_{shape}), and overall (Acc_{all}), making it suitable for human-centric evaluation. 3) Human Preference: we conduct a user study to evaluate the image quality and text-image alignment of each method.

5.2. Comparison to Text-to-Image Models

We compared our foundation model with various state-of-the-art text-to-image models, including open-source models like Stable Diffusion (SD-1.5/2.0), SDXL, DeepFloyd-IF, and commercial models such as DALLE2/3 and MidJourney. For a thorough comparison, we evaluated two versions of our foundation model: CosmicMan-SD based on SD-1.5 and CosmicMan-SXDL based on SDXL.

Quantitative Evaluation. We prepared a test set comprising 2048 human images with fine-grained manually annotated prompts for fine-grained text-image generation. We report the quantitative comparison in Tab. 2. CosmicMan-SDXL excels in both image quality (FID) and fine-grained text-image alignment (Acc_{all}). In terms of image genera-

tion quality, CosmicMan-SD/SDXL outperforms the corresponding SD-1.5/SDXL by a large margin, showing up to 23.52% and 27.13% relative improvements in FID. As for fine-grained text-image alignment, CosmicMan-SDXL demonstrates superior generative capabilities in terms of three types of descriptions: object, texture, and shape. Compared to DALLE-3, which also unleashes the potential of detailed descriptions, CosmicMan shows 7.54%, 1.38%, 15.97% and 7.46% relative performance boost on Acc_{obj}, Acc_{tex}, Acc_{shape} and Acc_{all}. Note that CosmicMan-SD/SDXL obtains a relatively low CLIPScore, as our emphasis was on evaluating fine-grained text-image alignment. In contrast, CLIPScore lacks the ability for fine-grained evaluation, consistent with the conclusions in the DSG [8] and GenEval [17]. CosmicMan-SD/SDXL achieves the best performance in Acc_{all} and human preference evaluation, indicating its superiority in 2D human image generation.

Human Preference Evaluation. We compared our results with DeepFloyd-IF, SDXL, DALLE3, and MidJourney through pairwise comparisons. The evaluation considered both image quality and text-image alignment, using 100 randomly selected prompts to generate corresponding images for each method. The evaluation results exhibits a significant preference, with over 93.06%, 82.93%, 78.13% and 70.43% of subjects favoring our results in terms of image quality, and 85.38%, 90.25%, 88.56% and 81.68% of subjects preferring our results over those of DeepFloyd-IF, SDXL, DALLE-3, and MidJourney in terms of text-image alignment. Qualitative results in the supplementary material further highlight our model’s superiority in image quality, fine-grained details, and text-image alignment.

5.3. Ablation Study

Ablation on Training Data. To show the validity of our proposed CosmicMan-HQ dataset, Tab. 3 reports the evaluation from three aspects: data source, data scale and annotation quality. 1) Data Source. Compared with two cutting-edge datasets, LAION-5B and HumanSD, *Ours* surpasses them by over 11.44 and 10.52 in FID, and 5.1 and 4.7 in Acc_{all}, respectively. LAION-5B has large noise in both data and annotation, while HumanSD has fewer data quantities

Table 3. **Ablation on Training Data.** “AltText” refers to Web Alternative Text, “IB_{pre}” denotes the image descriptions generated by the pretrained InstructBLIP model, and “Ours” corresponds to captions produced by Annotate Anyone (“AA”).

Dataset	Num	Text	FID↓	Acc _{all} ↑
LAION-5B	5B	AltText	48.09	74.6
HumanSD	1M	AltText	49.01	75.0
Ours-1	1M	AltText	47.65	75.2
Ours-2	1M	IB _{pre}	51.02	75.6
Ours-3	1M	AA	40.08	78.8
Ours	6M	AA	37.57	79.7

Table 4. **Ablation on Training Strategy.** “Baseline” refers to the SD pretrained model. “CMHQ” stands for CosmicMan-HQ.

Methods	FID↓	Acc _{obj} ↑	Acc _{tex} ↑	Acc _{shape} ↑	Acc _{all} ↑
Baseline	48.09	87.3	77.4	59.3	74.6
+ CMHQ	37.57	90.8	83.5	64.8	79.7
+ $\mathcal{L}_{\text{HOLA}}$	36.78	91.7	85.7	66.1	81.2

and coarse annotations. Owing to the scalable ability of our data production workflow, Annotate Anyone, the constructed CosmicMan-HQ dataset features a large quantity of high-quality annotations, which benefits the final results. 2) Data Scaling. *Ours*, trained with 6M images, brings a promotion of 2.51 in FID and 0.9 Acc_{all} compared to 1M version *Ours-3*, proving the effectiveness of data scaling. Thus, Annotate Anyone’s capacity to run constantly to produce data is necessary to push the boundaries of foundation models’ performance. 3) Annotation Quality. We make a comparison under three different caption settings. *Ours-3* with AA caption exhibits a significant improvement of 7.57 and 10.94 in FID, as well as 3.6 and 3.2 in Acc_{all} compared to *Ours-1* and *Ours-2*. This verifies the effectiveness of improving the annotation quality of our proposed human-in-the-loop annotation mechanism in Annotate Anyone.

Ablation on Training Strategy. Tab. 4 shows the ablation of the training dataset and model design used in CosmicMan. By leveraging our CosmicMan-HQ dataset, fine-tuning the model gains a promotion of 10.52 in FID and 6.3 in Acc_{all}. Our proposed $\mathcal{L}_{\text{HOLA}}$ further enhances FID and Acc_{all} by 0.79 and 1.5. Our novel perspectives on data and model design boost remarkable promotions of CosmicMan on fine-grained human generation.

5.4. Applications

To validate the effectiveness of our human-specialized foundation model, we conduct additional experiments on 2D and 3D human-centric applications.

2D Human Editing. 2D human editing manipulates human images for specified poses. We compare our CosmicMan-

Table 5. **Quantitative Comparison on 2D Human Editing and 3D Human Reconstruction.** User study reports the ratio of users who prefer our results to SD/SDXL.

2D Application	FID↓	Acc _{all} ↑	User Study
T2I-Adapter + SDXL	47.73	76.6	18.33%
T2I-Adapter + CosmicMan-SDXL	37.62	82.9	81.67%
3D Application	CLIP-Sim↑	Acc _{all} ↑	User Study
Magic123 + SD	0.83	67.6	26.36%
Magic123 + CosmicMan-SD	0.88	70.8	73.64%

SDXL with SDXL based on T2I-Adapter [41]. In Tab. 5, our model outperforms SDXL on both FID and Acc_{all}, showing its superiority in 2D human editing tasks.

3D Human Reconstruction. We validate the effectiveness of our CosmicMan-SD model based on Magic123 [47], one representative 3D object reconstruction method from a single image. We replace the SD pretrained model with our foundation model in Magic123 for comparison. The higher CLIP-similarity [47] and Acc_{all} in Tab. 5 exhibit the superior potential of our model on 3D human reconstruction.

6. Discussion

Release. We seriously treat the license and privacy issues and follow a rigorous legal review in our institute. CosmicMan-HQ 1.0 with all of the annotations will be released step by step. People in the dataset are anonymized without additional private or sensitive metadata. All released data are free for research use only. The model and codes will also be released.

Future Work. Not placing CosmicMan merely as a research paper, we also commit ourselves to providing a long-term and sustainable foundation platform to support the research in human-centric content generation. Thus, we will continuously 1) operate Annotate Anyone to produce subsequent versions of CosmicMan-HQ aligned dynamically with real-world data, and 2) provide up-to-date human-specialized foundation models periodically trained on new versions of our data. By providing a well-constructed and long-term-maintained infrastructure, we hope to benefit broader research communities centered on human subjects.

References

- [1] Harsh Agrawal, Karan Desai, Yufei Wang, Xinlei Chen, Rishabh Jain, Mark Johnson, Dhruv Batra, Devi Parikh, Stefan Lee, and Peter Anderson. nocaps: novel object captioning at scale. In *Proceedings of the IEEE International Conference on Computer Vision*, pages 8948–8957, 2019. 2
- [2] James Betker, Gabriel Goh, Li Jing, Tim Brooks, Jianfeng Wang, Linjie Li, Long Ouyang, Juntang Zhuang, Joyce Lee, Yufei Guo, et al. Improving image generation with better captions. 2023. 3, 4, 5, 8
- [3] Minwoo Byeon, Beomhee Park, Haecheon Kim, Sungjun

- Lee, Woonhyuk Baek, and Saehoon Kim. Coyo-700m: Image-text pair dataset. <https://github.com/kakaobrain/coyo-dataset>, 2022. 2
- [4] Zhe Cao, Tomas Simon, Shih-En Wei, and Yaser Sheikh. Realtime multi-person 2d pose estimation using part affinity fields. In *Proceedings of the IEEE conference on computer vision and pattern recognition*, pages 7291–7299, 2017. 24
- [5] Hila Chefer, Yuval Alaluf, Yael Vinker, Lior Wolf, and Daniel Cohen-Or. Attend-and-excite: Attention-based semantic guidance for text-to-image diffusion models. *ACM Transactions on Graphics (TOG)*, 42(4):1–10, 2023. 3
- [6] Junsong Chen, Jincheng Yu, Chongjian Ge, Lewei Yao, Enze Xie, Yue Wu, Zhongdao Wang, James Kwok, Ping Luo, Huchuan Lu, and Zhenguo Li. Pixart- α : Fast training of diffusion transformer for photorealistic text-to-image synthesis, 2023. 3, 4, 5
- [7] Wei Cheng, Ruixiang Chen, Siming Fan, Wanqi Yin, Keyu Chen, Zhongang Cai, Jingbo Wang, Yang Gao, Zhengming Yu, Zhengyu Lin, Daxuan Ren, Lei Yang, Ziwei Liu, Chen Change Loy, Chen Qian, Wayne Wu, Dahua Lin, Bo Dai, and Kwan-Yee Lin. Dna-rendering: A diverse neural actor repository for high-fidelity human-centric rendering. In *Proceedings of the IEEE/CVF International Conference on Computer Vision (ICCV)*, pages 19982–19993, 2023. 2
- [8] Jaemin Cho, Yushi Hu, Roopal Garg, Peter Anderson, Ranjay Krishna, Jason Baldridge, Mohit Bansal, Jordi Pont-Tuset, and Su Wang. Davidsonian scene graph: Improving reliability in fine-grained evaluation for text-image generation. *arXiv preprint arXiv:2310.18235*, 2023. 8, 18
- [9] Wenliang Dai, Junnan Li, Dongxu Li, Anthony Meng Huat Tiong, Junqi Zhao, Weisheng Wang, Boyang Li, Pascale Fung, and Steven Hoi. Instructblip: Towards general-purpose vision-language models with instruction tuning, 2023. 5, 13, 14, 17
- [10] Xiaoliang Dai, Ji Hou, Chih-Yao Ma, Sam Tsai, Jialiang Wang, Rui Wang, Peizhao Zhang, Simon Vandenhende, Xiaofang Wang, Abhimanyu Dubey, et al. Emu: Enhancing image generation models using photogenic needles in a haystack. *arXiv preprint arXiv:2309.15807*, 2023. 18
- [11] DeepFloyd. Deepfloyd-if, 2023. 3, 8
- [12] Jia Deng, Wei Dong, Richard Socher, Li-Jia Li, Kai Li, and Li Fei-Fei. Imagenet: A large-scale hierarchical image database. In *2009 IEEE conference on computer vision and pattern recognition*, pages 248–255. Ieee, 2009. 4
- [13] Patrick Esser, Robin Rombach, and Björn Ommer. Taming transformers for high-resolution image synthesis, 2020. 2
- [14] Weixi Feng, Xuehai He, Tsu-Jui Fu, Varun Jampani, Arjun Reddy Akula, Pradyumna Narayana, Sugato Basu, Xin Eric Wang, and William Yang Wang. Training-free structured diffusion guidance for compositional text-to-image synthesis. In *The Eleventh International Conference on Learning Representations*, 2023. 3
- [15] Flickr. Flickr application programming interface (api), 2023. Accessed: 2023-11-18. 4
- [16] Jianglin Fu, Shikai Li, Yuming Jiang, Kwan-Yee Lin, Chen Qian, Chen Change Loy, Wayne Wu, and Ziwei Liu. Stylegan-human: A data-centric odyssey of human generation. In *European Conference on Computer Vision*, pages 1–19. Springer, 2022. 2, 3, 4, 6, 13
- [17] Dhruva Ghosh, Hanna Hajishirzi, and Ludwig Schmidt. Geneval: An object-focused framework for evaluating text-to-image alignment. *arXiv preprint arXiv:2310.11513*, 2023. 3, 8
- [18] Honglin He, Zhuoqian Yang, Shikai Li, Bo Dai, and Wayne Wu. Orthoplanes: A novel representation for better 3d-awareness of gans. In *Proceedings of the IEEE/CVF International Conference on Computer Vision (ICCV)*, pages 22996–23007, 2023. 2
- [19] Amir Hertz, Ron Mokady, Jay Tenenbaum, Kfir Aberman, Yael Pritch, and Daniel Cohen-Or. Prompt-to-prompt image editing with cross attention control. *arXiv preprint arXiv:2208.01626*, 2022. 3, 19
- [20] Jack Hessel, Ari Holtzman, Maxwell Forbes, Ronan Le Bras, and Yejin Choi. Clipscore: A reference-free evaluation metric for image captioning. *arXiv preprint arXiv:2104.08718*, 2021. 8
- [21] Martin Heusel, Hubert Ramsauer, Thomas Unterthiner, Bernhard Nessler, and Sepp Hochreiter. Gans trained by a two time-scale update rule converge to a local nash equilibrium. *Advances in neural information processing systems*, 30, 2017. 8
- [22] Jonathan Ho, Ajay Jain, and Pieter Abbeel. Denoising diffusion probabilistic models. *arXiv preprint arxiv:2006.11239*, 2020. 2, 18
- [23] Kaiyi Huang, Kaiyue Sun, Enze Xie, Zhenguo Li, and Xi-hui Liu. T2i-compench: A comprehensive benchmark for open-world compositional text-to-image generation. *arXiv preprint arXiv:2307.06350*, 2023. 3, 8, 18
- [24] Tanuj Jain, Christopher Lennan, Zubin John, and Dat Tran. Imagededup. <https://github.com/idealoid/imagededup>, 2019. 13
- [25] Menglin Jia, Mengyun Shi, Mikhail Sirotenko, Yin Cui, Claire Cardie, Bharath Hariharan, Hartwig Adam, and Serge Belongie. Fashionpedia: Ontology, segmentation, and an attribute localization dataset. In *Computer Vision—ECCV 2020: 16th European Conference, Glasgow, UK, August 23–28, 2020, Proceedings, Part I 16*, pages 316–332. Springer, 2020. 13
- [26] Yuming Jiang, Shuai Yang, Haonan Qiu, Wayne Wu, Chen Change Loy, and Ziwei Liu. Text2human: Text-driven controllable human image generation. *ACM Transactions on Graphics (TOG)*, 41(4):1–11, 2022. 2, 3, 6
- [27] Byungho Jo, Donghyeon Cho, In Kyu Park, and Sungeun Hong. Ifqa: Interpretable face quality assessment. In *Proceedings of the IEEE/CVF Winter Conference on Applications of Computer Vision*, pages 3444–3453, 2023. 4
- [28] Xuan Ju, Ailing Zeng, Jianan Wang, Qiang Xu, and Lei Zhang. Human-art: A versatile human-centric dataset bridging natural and artificial scenes. In *Proceedings of the IEEE/CVF Conference on Computer Vision and Pattern Recognition*, pages 618–629, 2023. 4, 6
- [29] Xuan Ju, Ailing Zeng, Chenchen Zhao, Jianan Wang, Lei Zhang, and Qiang Xu. Humansd: A native skeleton-guided diffusion model for human image generation. *arXiv preprint arXiv:2304.04269*, 2023. 2, 3, 5, 6

- [30] Junnan Li, Dongxu Li, Caiming Xiong, and Steven Hoi. Blip: Bootstrapping language-image pre-training for unified vision-language understanding and generation. In *International Conference on Machine Learning*, pages 12888–12900. PMLR, 2022. 14, 17
- [31] Peike Li, Yunqiu Xu, Yunchao Wei, and Yi Yang. Self-correction for human parsing. *IEEE Transactions on Pattern Analysis and Machine Intelligence*, 44(6):3260–3271, 2020. 5
- [32] Yumeng Li, Margret Keuper, Dan Zhang, and Anna Khoreva. Divide and bind your attention for improved generative semantic nursing, 2023. 3
- [33] Anran Lin, Nanxuan Zhao, Shuliang Ning, Yuda Qiu, Baoyuan Wang, and Xiaoguang Han. Fashiontext: Controllable virtual try-on with text and texture. In *ACM SIGGRAPH 2023 Conference Proceedings*, 2023. 2, 3
- [34] Baijiong Lin, Feiyang Ye, Yu Zhang, and Ivor W Tsang. Reasonable effectiveness of random weighting: A litmus test for multi-task learning. *arXiv preprint arXiv:2111.10603*, 2021. 18
- [35] Tsung-Yi Lin, Michael Maire, Serge Belongie, James Hays, Pietro Perona, Deva Ramanan, Piotr Dollár, and C. Lawrence Zitnick. Microsoft coco: Common objects in context. In *ECCV 2014*, 2014. 2, 4, 23
- [36] Ruoshi Liu, Rundi Wu, Basile Van Hoorick, Pavel Tokmakov, Sergey Zakharov, and Carl Vondrick. Zero-1-to-3: Zero-shot one image to 3d object. In *Proceedings of the IEEE/CVF International Conference on Computer Vision*, pages 9298–9309, 2023. 2, 3
- [37] Ziwei Liu, Ping Luo, Shi Qiu, Xiaogang Wang, and Xiaoou Tang. Deepfashion: Powering robust clothes recognition and retrieval with rich annotations. In *Proceedings of the IEEE conference on computer vision and pattern recognition*, pages 1096–1104, 2016. 4, 13
- [38] Ilya Loshchilov and Frank Hutter. Decoupled weight decay regularization. *arXiv preprint arXiv:1711.05101*, 2017. 8
- [39] Midjourney. Midjourney, 2023. 2, 8
- [40] Davide Morelli, Alberto Baldrati, Giuseppe Cartella, Marcella Cornia, Marco Bertini, and Rita Cucchiara. LaD-VTON: Latent Diffusion Textual-Inversion Enhanced Virtual Try-On. In *Proceedings of the ACM International Conference on Multimedia*, 2023. 3
- [41] Chong Mou, Xintao Wang, Liangbin Xie, Jian Zhang, Zhonggang Qi, Ying Shan, and Xiaohu Qie. T2i-adapter: Learning adapters to dig out more controllable ability for text-to-image diffusion models. *arXiv preprint arXiv:2302.08453*, 2023. 3, 9, 24, 27
- [42] Martin Pernuš, Clinton Fookes, Vitomir Štruc, and Simon Dobrišek. Fice: Text-conditioned fashion image editing with guided gan inversion, 2023. 3
- [43] Pixabay. Pixabay application programming interface (api), 2023. Accessed: 2023-11-18. 4
- [44] Bryan A. Plummer, Liwei Wang, Chris M. Cervantes, Juan C. Caicedo, Julia Hockenmaier, and Svetlana Lazebnik. Flickr30k entities: Collecting region-to-phrase correspondences for richer image-to-sentence models, 2016. 2
- [45] Dustin Podell, Zion English, Kyle Lacey, Andreas Blattmann, Tim Dockhorn, Jonas Müller, Joe Penna, and Robin Rombach. Sdxl: improving latent diffusion models for high-resolution image synthesis. *arXiv preprint arXiv:2307.01952*, 2023. 2, 3, 8, 18
- [46] Ben Poole, Ajay Jain, Jonathan T Barron, and Ben Mildenhall. Dreamfusion: Text-to-3d using 2d diffusion. *arXiv preprint arXiv:2209.14988*, 2022. 2, 3
- [47] Guocheng Qian, Jinjie Mai, Abdullah Hamdi, Jian Ren, Aliaksandr Siarohin, Bing Li, Hsin-Ying Lee, Ivan Skokhodov, Peter Wonka, Sergey Tulyakov, et al. Magic123: One image to high-quality 3d object generation using both 2d and 3d diffusion priors. *arXiv preprint arXiv:2306.17843*, 2023. 9, 24, 28
- [48] Aditya Ramesh, Mikhail Pavlov, Gabriel Goh, Scott Gray, Chelsea Voss, Alec Radford, Mark Chen, and Ilya Sutskever. Zero-shot text-to-image generation. In *Proceedings of the International Conference on Machine Learning*, pages 8821–8831, 2021. 2, 3
- [49] Aditya Ramesh, Prafulla Dhariwal, Alex Nichol, Casey Chu, and Mark Chen. Hierarchical text-conditional image generation with clip latents, 2022. 3, 8
- [50] Royi Rassin, Eran Hirsch, Daniel Glickman, Shauli Ravfogel, Yoav Goldberg, and Gal Chechik. Linguistic binding in diffusion models: Enhancing attribute correspondence through attention map alignment, 2023. 3
- [51] Robin Rombach, Andreas Blattmann, Dominik Lorenz, Patrick Esser, and Björn Ommer. High-resolution image synthesis with latent diffusion models. In *Proceedings of the IEEE/CVF conference on computer vision and pattern recognition*, pages 10684–10695, 2022. 2, 3, 8, 18
- [52] Nataniel Ruiz, Yuanzhen Li, Varun Jampani, Yael Pritch, Michael Rubinstein, and Kfir Aberman. Dreambooth: Fine tuning text-to-image diffusion models for subject-driven generation. In *Proceedings of the IEEE/CVF Conference on Computer Vision and Pattern Recognition (CVPR)*, pages 22500–22510, 2023. 2
- [53] Chitwan Saharia, William Chan, Saurabh Saxena, Lala Li, Jay Whang, Emily Denton, Seyed Kamyar Seyed Ghasemipour, Raphael Gontijo-Lopes, Burcu Karagol Ayan, Tim Salimans, Jonathan Ho, David J. Fleet, and Mohammad Norouzi. Photorealistic text-to-image diffusion models with deep language understanding. In *Advances in Neural Information Processing Systems*, 2022. 2, 3
- [54] Shunsuke Saito, Zeng Huang, Ryota Natsume, Shigeo Morishima, Angjoo Kanazawa, and Hao Li. Pifu: Pixel-aligned implicit function for high-resolution clothed human digitization. *arXiv preprint arXiv:1905.05172*, 2019. 2
- [55] Christoph Schuhmann, Romain Beaumont, Richard Vencu, Cade Gordon, Ross Wightman, Mehdi Cherti, Theo Coombes, Aarush Katta, Clayton Mullis, Mitchell Wortsman, et al. Laion-5b: An open large-scale dataset for training next generation image-text models. *Advances in Neural Information Processing Systems*, 35:25278–25294, 2022. 2, 4, 13
- [56] Piyush Sharma, Nan Ding, Sebastian Goodman, and Radu Soricut. Conceptual captions: A cleaned, hypernymed, im-

- age alt-text dataset for automatic image captioning. In *Proceedings of ACL*, 2018. 2
- [57] Oleksii Sidorov, Ronghang Hu, Marcus Rohrbach, and Amanpreet Singh. Textcaps: a dataset for image captioning with reading comprehension. 2020. 2
- [58] Quan Sun, Yuxin Fang, Ledell Wu, Xinlong Wang, and Yue Cao. Eva-clip: Improved training techniques for clip at scale. *arXiv preprint arXiv:2303.15389*, 2023. 4
- [59] Unsplash. Unsplash application programming interface (api), 2023. Accessed: 2023-11-18. 4
- [60] Aaron van den Oord, Oriol Vinyals, and koray kavukcuoglu. Neural discrete representation learning. In *Advances in Neural Information Processing Systems*, 2017. 2, 3
- [61] Chien-Yao Wang, Alexey Bochkovskiy, and Hong-Yuan Mark Liao. Yolov7: Trainable bag-of-freebies sets new state-of-the-art for real-time object detectors. In *Proceedings of the IEEE/CVF Conference on Computer Vision and Pattern Recognition*, pages 7464–7475, 2023. 5
- [62] Luozhou Wang, Guibao Shen, Yijun Li, and Yingcong Chen. Decompose and realign: Tackling condition misalignment in text-to-image diffusion models, 2023. 3
- [63] Xiaoshi Wu, Yiming Hao, Keqiang Sun, Yixiong Chen, Feng Zhu, Rui Zhao, and Hongsheng Li. Human preference score v2: A solid benchmark for evaluating human preferences of text-to-image synthesis. *arXiv preprint arXiv:2306.09341*, 2023. 4, 8
- [64] Guangxuan Xiao, Tianwei Yin, William T Freeman, Frédo Durand, and Song Han. Fastcomposer: Tuning-free multi-subject image generation with localized attention. *arXiv preprint arXiv:2305.10431*, 2023. 3
- [65] Zhen Xu, Sida Peng, Haotong Lin, Guangzhao He, Jiaming Sun, Yujun Shen, Hujun Bao, and Xiaowei Zhou. 4k4d: Real-time 4d view synthesis at 4k resolution. 2023. 2
- [66] Zhuoqian Yang, Shikai Li, Wayne Wu, and Bo Dai. 3dhuman: 3d-aware human image generation with 3d pose mapping. In *Proceedings of the IEEE/CVF International Conference on Computer Vision (ICCV)*, pages 23008–23019, 2023. 2
- [67] Lvmin Zhang, Anyi Rao, and Maneesh Agrawala. Adding conditional control to text-to-image diffusion models. In *Proceedings of the IEEE/CVF International Conference on Computer Vision (ICCV)*, pages 3836–3847, 2023. 2, 3
- [68] Weixia Zhang, Guangtao Zhai, Ying Wei, Xiaokang Yang, and Kede Ma. Blind image quality assessment via vision-language correspondence: A multitask learning perspective. In *Proceedings of the IEEE/CVF Conference on Computer Vision and Pattern Recognition*, pages 14071–14081, 2023. 4
- [69] Xujie Zhang, Binbin Yang, Michael C. Kampffmeyer, Wenqing Zhang, Shiyue Zhang, Guansong Lu, Liang Lin, Hang Xu, and Xiaodan Liang. Diffcloth: Diffusion based garment synthesis and manipulation via structural cross-modal semantic alignment. In *Proceedings of the IEEE/CVF International Conference on Computer Vision (ICCV)*, pages 23154–23163, 2023. 3
- [70] Yutong Zhou and Nobutaka Shimada. Generative adversarial network for text-to-face synthesis and manipulation with pre-trained bert model. In *2021 16th IEEE International Conference on Automatic Face and Gesture Recognition (FG 2021)*, pages 01–08, 2021. 4

Appendix

This appendix serves to further enrich the discourse established in our main paper. In Sec. A, we present additional elaboration on the scalable data production pipeline – Annotate Anyone. Then, in Sec. B, we delve into the proposed training framework (*i.e.*, Daring) with additional evaluation and illustrations. Lastly, we present a broader range of qualitative results, including comparisons with state-of-the-art methods, more examples of generated samples, extensive ablation studies, and potential application demonstrations in Sec. C.

A. Annotate Anyone

As introduced in the main paper, the whole data production paradigm comprises two parts that benefit from the cooperation of human effort and AI models – a flowing data sourcing for data collection, and human-in-the-loop data annotation. In this section, we unfold the details of Annotate Anyone. We first complement the data filtering step in Sec. A.1. Then, we provide the pseudo-code for fine-tuning the VLM model used in Annotate Anyone, accompanied by an exhaustive explanation (Sec. A.2). Besides, we conduct experiments to demonstrate the effectiveness of the proposed human-in-the-loop annotation pipeline in Sec. A.3. Moreover, we provide a detailed exposition of all 70 questions we used on VLM for obtaining the description of an image, as presented in Sec. A.4. We also list the corresponding attribute labels extracted from the output of VLM models. Finally, a detailed statistical analysis (Sec. A.5) and additional data samples from our dataset CosmicMan-HQ 1.0 (Sec. A.6) are presented.

Algorithm 1 Annotate Anyone:

Iteratively improve VLM model to annotate image

Input: I ▷ Images in Data Pool
 $I_0 \leftarrow$ sample test set from I ▷ K images
 $A_0 \leftarrow$ label I_0 by VQA pretrained model (IB_0)
 $M_0 \leftarrow$ label I_0 by human
 $Acc \leftarrow$ Eval(A_0, M_0) ▷ Acc for all label
 $i = 0$
while $Acc < 85\%$ **do**
 $i \leftarrow i + 1$
 $I_i \leftarrow$ sample K images from data pool
 $\tilde{M}_i \leftarrow$ select labels from M_i with $Acc < 85\%$
 $IB_{i+1} \leftarrow$ finetune IB_i with $(\cup_1^i \tilde{M}_i, I_i)$
 $A_{i+1} \leftarrow$ label I_0 by (IB_{i+1})
 $Acc \leftarrow$ Eval(A_{i+1}, M_0)
end while
 $(I, A) \leftarrow$ update all image label in data pool using IB_{i+1}

A.1. Data Filtering

As mentioned in the main text, we use three academic datasets, LAION-5B [55], SHHQ [16], and DeepFashion [37] as part of data origin. When distilling LAION-5B dataset, we extensively utilize the meta information provided by LAION-5B itself to perform an initial screening of the data. We filter out a significant amount of images that contain the “Not safe for work (nsfw)” label or have a watermark score higher than 0.5. The data source of SHHQ and DeepFashion is relatively concentrated, consisting exclusively of watermark-free fashion / studio-shot data. Thus, we omit this step for those two datasets. Before fetching images from the Internet, we excluded the data origins of LAION-5B, SHHQ, and DeepFashion. Our aim is to minimize crawling data from the same source as much as possible. We also remove duplicated images by encoding images into fixed-length hash values using perceptual hashing algorithms [24]. Images with hamming distances smaller than 3 are considered duplicates, and one of them will be removed to avoid redundancy.

A.2. Human-in-the-loop Data Annotation

This section presents the pseudo-code of the annotation algorithm (see Algorithm. 1) mentioned in Sec. 3.2.2 of the main text for Annotate Anyone. A detailed step-by-step explanation will be provided below.

The overall objective of this process is to achieve collaboration between AI and human to provide descriptions for all images (denoted as I) within the entire data pool. We start the workflow by randomly selecting a fixed test set I_0 , consisting of K images from the data pool I . I_0 will be asked 70 meticulously crafted vision questions (see Tab. 6 for reference) by the pretrained model IB_0 [9] and obtain corresponding answers A_0 . Note that, inspired by the annotation approach used in Fashion datasets [25, 37], we transform the uncontrollable, attributes highly entangled captioning tasks into detailed question-answering tasks to get A_0 . This approach results in structured label answers, proceeding from coarse to finer granularity, that can ease evaluation and provide more accurate and fine-grained region-specific labels. Then, we ask a professional annotation team to manually label the images in I_0 based on these 70 questions, to form the attribute dictionary M_0 as the ground-truth of the test set. For every single question, we evaluate the accuracy of the pretrained model IB_0 by comparing the label in A_0 and M_0 .

The label accuracy for every attribute corresponding to every question will be documented and utilized to assess whether the current (pretrained and fine-tuned) model’s judgment for that attribute meets the criteria. If there is one label’s accuracy less than 85%, the fine-tuning loop of AI model IB starts. Concretely, We will randomly sample another K images from the data pool, and ask the annota-

				
Raw Text	Flora and Fauna Dress	Best of Christmas Project	Alexa Mansour as Hope - The Walking Dead: World Beyond _ Season 1, Episode 1 - Photo Credit: Zach Dilgard/AMC	-
BLIP	a woman wearing a leopard print dress and a hat	there is a little girl sitting on a rug with a toothbrush	a woman sitting in a chair in a kitchen	a woman in a short dress holding an umbrella
InstructBlip	the leopard off the shoulder dress	The person in the picture is a young girl sitting on the floor next to a Christmas tree, playing with a toy.	The image features a woman sitting on a chair in a living room. She is wearing jeans and a sweater, with her hands resting on her knees. There are several objects scattered around the room, including a vase, a cup, and a bottle of wine.	The image depicts a young woman standing under an umbrella in a park. She is wearing a black skirt and white top, while holding an umbrella to protect herself from the sun.
Ours	A nearly full-body shot, a Caucasian adult female, fit, indoor, wavy above chest brown hair, woven hat, cotton graphic medium sleeve short off-shoulder dress	A nearly full-body shot, a Caucasian child female, fit, indoor, cotton short sleeve dress in red, long sleeve cotton stripes shirt, bob blonde above shoulders hair	A nearly full-body shot, an middle eastern female, fit, indoor, black wavy hair above the chest. Cotton short sleeve t-shirt in gray with a v-shape neckline, blue denim jeans with maxi length	A full-body shot, an Asian adult female, outdoor, black straight above chest hair, a black silk shirt with long sleeve and collar, cotton white and short pleated skirt, black leather loafers, white cotton socks

Figure 1. **Data and Annotation Samplings.** Sample images with captions obtained from different methods: the original text uploaded along with the images, captions generated by BLIP [30], and InstructBLIP [9] pretrained models, and our attribute-based text. Here we use different colors to highlight the unrelated, wrong, and coarse and vague descriptions.

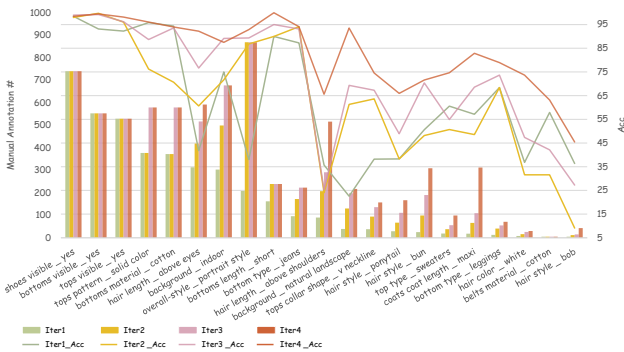


Figure 2. **Effectiveness of Annotate Anyone.** The bar charts represent the manual annotation counts for different attributes in 1000 images for each iteration, and the solid lines depict the accuracy of each attribute under the current model. Better zoom in for details.

tion team to label the attributes whose model accuracy is less than 85%. After each round of manual annotation, the newly manual-labeled data is combined with the previously annotated data and utilized for fine-tuning the IB_i model. During training, we use “<Image>: {}. Question: {} Answer:” as a template to construct fine-tuning dataset. The fine-tuned model IB_{i+1} will be utilized to perform infer-

ence on the test set I_0 for evaluation to get Acc . This fine-tuning process will repeat until the overall label accuracy achieves 85%. The final model IB_{i+1} is used to annotate all the images in the data pool, and results image-label pairs (I, A) .

A.3. Effectiveness of Annotate Anyone

In this section, we conduct experiments to assess the effectiveness of reducing manual annotation efforts in our Annotate Anyone pipeline.

We run four sets of model fine-tuning with a step-wise augmentation of manually labeled data. In every iteration, we randomly sampled 1000 images (K in Algorithm. 1 is set to 1000) from I in the data pool. Leveraging evaluation metrics (Acc) from the previous model, we progressively decrease the need for manual labeling by excluding already qualified attributes (where the Acc is higher than 85%). The annotated data accumulates and is utilized for fine-tuning the subsequent model.

As shown in bar charts of the first iteration in Fig. 2, due to the random sampling from the data pool, the inherent attribute distribution of sampled images naturally exhibits a long-tail pattern similar to that of CosmicMan-HQ

Table 6. **The Detailed Questions Asked to Describe Every Single Image.** The index 0-2 in Acc represents the corresponding questions is evaluated as **Acc_{obj}**, **Acc_{tex}**, and **Acc_{shape}**.

	Q _{idx}	Acc	Questions	Attributes
Overall	1	0	what is the gender of the person in the image?	male, female
	2	0	what is the country of the person in the image?	Indian, Latino, Middle Eastern, ...
	3	0	what is the age of the person in the image?	teenager, adult, elderly, ...
	4	0	what is the body shape of the person in the image?	fit, skinny, obese, muscular
	5	0	what is the background of the person in the image?	
	6	0	what is the overall-style of the person in the image?	fashion, documentary, portrait, others
Hair	7	0	is the hair of the person visible in the image?	yes, no
	8	-	what is the hair color of the person?	brown, gray, violet, ...
	9	1	what is the hairstyle of the person?	wavy, ponytail, straight, ...
	10	2	what is the hair length of the person?	below chest, bald, bob, ...
Top Clothings	11	0	does the person wears any tops?	yes, no
	12	0	what kind of top does the person wear?	vest, blouse, hoodie, ...
	13	1	what is the pattern of the tops?	graphic, printed, stripes, ...
	14	1	what is the material of the tops?	linen, fur, lace, ...
	15	2	what is the sleeve length of the tops?	short, medium, sleeveless, ...
	16	2	what is the top length of the tops?	crop, normal, tunic
	17	2	what is the collar shape of the tops?	square, v-shape, collar, ...
	18	-	are the top clothing {random color}?	yes, no
Bottom Clothings	19	0	does the person wears any bottoms?	yes, no
	20	0	what kind of bottom does the person wear?	shorts, sweatpants, skirt, ...
	21	1	what is the pattern of the bottoms?	graphic, printed, stripes, ...
	22	1	what is the material of the bottoms?	linen, fur, lace, ...
	23	2	what is the length of the bottoms?	short, medium, sleeveless, ...
	24	2	what is the bottom shape of the bottoms?	straight, tapered, wide-leg, ...
One-piece Outfits	25	-	are the bottom clothing {random color}?	yes, no
	26	0	does the person wears any one-piece outfits?	yes, no
	27	0	what kind of one-piece outfit does the person wear?	bathrobe, jumpsuit, dress, ...
	28	1	what is the pattern of the one-piece outfits?	graphic, printed, stripes, ...
	29	1	what is the material of the one-piece outfits?	linen, fur, lace, ...
	30	2	what is the sleeve length of the one-piece outfits?	short, medium, sleeveless, ...
	31	2	what is the collar shape of the one-piece outfits?	square, v-shape, collar, ...
Coats	32	2	what is the length of the one-piece outfits?	short, medium, sleeveless, ...
	33	2	what is the shoulder exposure level of the one-piece outfits?	one-shoulder, off-shoulder
	34	0	does the person wears any coats?	yes, no
	35	0	what kind of coat does the person wear?	cape, trench coat, blazer, ...
	36	1	what is the pattern of the coats?	graphic, printed, stripes, ...
	37	1	what is the material of the coats?	linen, fur, lace, ...
	38	2	what is the coat length of the coats?	short, medium, maxi
	39	2	what is the collar shape of the coats?	square, v-shape, collar, ...
Special Clothings	40	-	are the coat {random color}?	yes, no
	41	0	does the person wears any special clothings?	yes, no
	42	0	what kind of special clothing does the person wear?	Hanfu, Saree, cosplay, ...
Shoes	43	2	what is the sleeve length of the special clothing?	short, medium, sleeveless, ...
	44	0	does the person wears any shoes?	yes, no
	45	0	what kind of shoe does the person wear?	sneakers, flip flops, loafers, ...
	46	1	what is the pattern of the shoes?	graphic, printed, stripes, ...
	47	1	what is the material of the shoes?	linen, fur, lace, ...
Bags	48	2	what is the boots length of the shoes?	ankle, mid-calf, knee-high, ...
	49	-	are the shoes {random color}?	yes, no
	50	0	does the person wears any bags?	yes, no
Hats	51	0	what is the type of the bags?	tote bag, handbag, wallet, ...
	52	1	what is the material of the bags?	linen, fur, lace, ...
	53	0	does the person wears any hats?	yes, no
Socks	54	0	what is the type of the hats?	beret, sun hat, helmet, ...,
	55	1	what is the material of the hats?	linen, fur, lace, ...
Other Accessories	56	1	what is the pattern of the socks?	graphic, printed, stripes, ...
	57	1	what is the material of the socks?	linen, fur, lace, ...
	58	1	what is the pattern of the belts?	graphic, printed, stripes, ...
	59	1	what is the material of the scarf?	linen, fur, lace, ...
	60	1	what is the pattern of the scarf?	graphic, printed, stripes, ...
Headwear	61	1	what is the material of the ties?	linen, fur, lace, ...
	62	1	what is the pattern of the ties?	graphic, printed, stripes, ...
	63	0	does the person wears any headwear?	yes, no
	64	0	what kind of headwear does the person wear?	headband, headscarf, veil
	65	1	what is the pattern of the headband?	graphic, printed, stripes, ...
	66	1	what is the material of the headband?	linen, fur, lace, ...
	67	1	what is the pattern of the headscarf?	graphic, printed, stripes, ...
68	1	what is the material of the headscarf?	linen, fur, lace, ...	
69	1	what is the pattern of the veil?	graphic, printed, stripes, ...	
70	1	what is the material of the veil?	linen, fur, lace, ...	

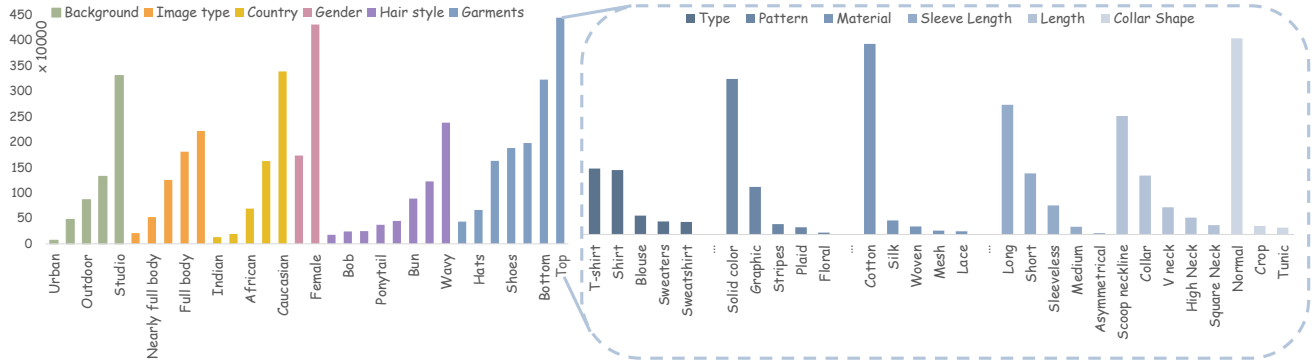


Figure 3. **CosmicMan-HQ 1.0 Statistics.** The left part shows the global attributes and garment types of the person in the image, and the right section displays attributes examples of top garments.

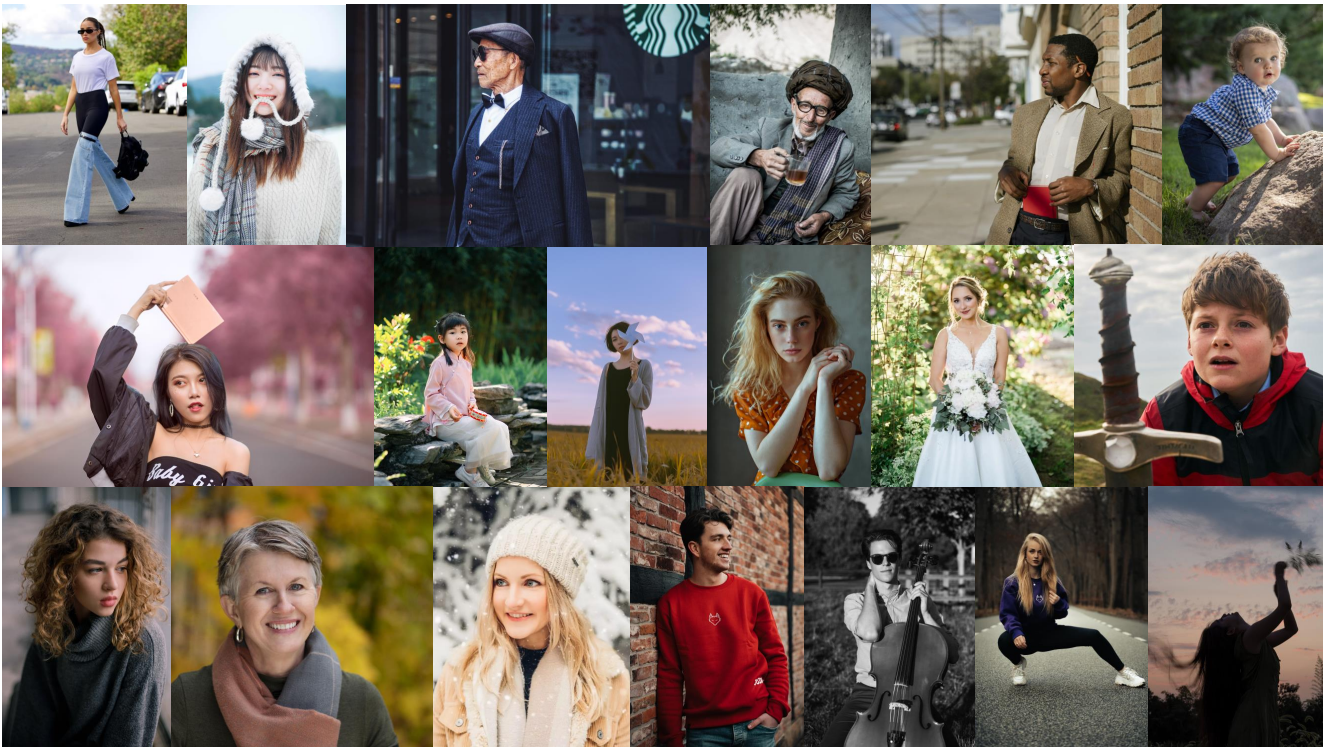


Figure 4. **CosmicMan-HQ 1.0 Image Examples.** The examples display the dataset’s wide-ranging diversity, encompassing different aspects like age, ethnicity, and clothing styles.

1.0 (Fig. 3). The accuracy of different attributes also correlates to the number of training data. Then in the following iterations, as we only augment the attributes that did not meet the accuracy threshold, the long-tail distribution of the training data is alleviated, as shown in the bar charts of Fig. 2. Specifically, with the progression of iterations, the number of labels requiring manual annotation on each image gradually decreases. Results in the figure showcase that the tail-end labels have improved over iterations while the existing qualified labels maintain their accuracy. The overall accuracy of the final fine-tuned model has significantly

increased from 56.0% in the pre-training phase to 85.3%. We have temporarily halted this flywheel because the average accuracy has reached 85%, but it can continue run until the accuracy of every single attribute meets the standard.

A.4. Label Protocol

In Tab. 6, we present a series of questions related to each part from the human parsing map, resulting in a total of 70 question-answer pairs to describe a human image.

A.5. Statistics of CosmicMan-HQ 1.0

To visually demonstrate the superiority of our dataset in terms of caption granularity and accuracy, Fig. 1 presents images from CosmicMan-HQ 1.0 paired with annotations from different sources. As shown, the text, including the raw caption from original websites and generated caption from the BLIP [30], often lacks descriptive details. Raw text is often unrelated to the image content, while text generated by BLIP is correct in general but vague, and the captions from the InstructBLIP [9] have lower accuracy in providing detailed captions, particularly in attribute-level descriptions. For example, InstructBLIP incorrectly stated that the woman is wearing a sweater instead of a short-sleeved shirt, as shown in the description of the third image in Fig. 1. Compared to these captions, our method provides comprehensive and accurate descriptions by transforming fine-grained labels using the fine-tuned IB model.

Following that, we delve into an in-depth exploration of the data distribution within the dataset. The statistical analysis of the overall image and human-centric attributes across CosmicMan-HQ 1.0 is displayed in the left half of Fig. 3. The right half offers examples of fine-grained attributes related to “top clothing”, which further demonstrates the granularity of our annotation. The histogram presents a wide coverage of various attributes and a natural long-tail distribution, which reflects our dataset’s consistency with the data in the real world.

A.6. More Dataset Samples

In Fig. 4, more image examples are randomly sampled from CosmicMan-HQ 1.0, which showcases the dataset’s inherent diversity across various dimensions, such as age, ethnicity, and garments.

B. Daring

In this section, we primarily focus on the additional analysis of our proposed training framework, *Daring*. Regarding the Data Discretization, we supplement with an ablation study on the type of captions, validating the effectiveness of the decomposed text space in Sec. B.1. We then provide a comparison on the two terms of the proposed HOLA loss in Sec. B.2. By presenting the cross-attention maps of the proposed model, we elucidate that our method improves the text-image alignment for dense concepts in Sec. B.3. We also conduct an experimental evaluation of optimization strategies involving different loss functions in Sec. B.4.

B.1. Evaluation of Data Discretization

Our framework first decomposes both the text and image into several groups of pair data. The underlying motivation is that we hypothesize the descriptions are decomposable and finite for describing human images, since

they are inherently associated with human body structure, and each concept can correspond to a particular body region. To evaluate the effectiveness of Data Discretization, we conduct an experiment on decomposed and continuous text space as shown in Tab. 7. Of note, to cost-effective get natural continuous text, we use GPT-4 to generate 5-10 templates for each set of labels in the human structure, such as: “{type} with {pattern} made of {material}, {sleeve_length} sleeves, {collar_shape} neckline, {length} length, {shoulder_exposure_level} exposure” for “One-piece Outfits” group. The natural descriptions of each group are concatenated to get a sentence for training and testing. Since the text encoder of SD can only handle 77 tokens, we construct another test set with short captions. For each sample within the original test set, when the number of tokens within the natural description is greater than 77, we randomly dropout descriptions of certain body parts. It can be seen that with the decomposed text data, the Acc_{all} exhibits a significant improvement. This is because decomposed text space ensures that all important details are accurately and clearly included and does not introduce ambiguity or unnecessary context. While data discretization gives an additional boost in performance, the best performance is achieved when $\mathcal{L}_{\text{HOLA}}$ and data discretization are combined. This illustrates that as long as keys K in attention blocks are initially decomposable and semantically guided, it may not be necessary to optimize latent code using cross-attention maps in the inference or add complex modules to SD’s original architecture for dense concepts alignment.

Table 7. **Ablation on $\mathcal{L}_{\text{HOLA}}$ and Data Discretization.** The best results are marked with Red.

$\mathcal{L}_{\text{HOLA}}$	Discretization	$\text{Acc}_{\text{obj}} \uparrow$	$\text{Acc}_{\text{tex}} \uparrow$	$\text{Acc}_{\text{shape}} \uparrow$	$\text{Acc}_{\text{all}} \uparrow$
		74.6	88.4	56.2	73.1
✓		76.8	89.3	59.3	75.1
	✓	82.4	91.3	66.5	80.1
✓	✓	85.5	92.2	71.4	83.1

B.2. Evaluation of HOLA Loss

The proposed loss $\mathcal{L}_{\text{HOLA}}$ for guiding the model to align with the region-level captions is composed of two terms. The first term introduces the overall spatial structure and single concept, while the second term reduces the ambiguities of outfit-level descriptions. For example, patterns exhibited on clothing typically manifest in specific areas rather than uniformly across the entire garment. Consequently, these patterns do not necessitate alignment across the entire clothing piece. Here we also provide quantitative results in Tab. 8. Baseline means the model that only fine-tuned on CosmicMan-HQ-1M. The employment of “term1” markedly enhances all semantic accuracy. Subsequent incorporation of “term2” yielded a more pronounced en-

hancement in Acc_{tex} due to the fact that certain outfit-level texture attributes such as patterns don’t need to be aligned with the whole semantic region.

Table 8. **Ablation on Loss Terms in $\mathcal{L}_{\text{HOLA}}$.** Term1 pushes the high response region of each single concept feature. Term2 helps reduce the ambiguities of outfit-level descriptions.

Methods	$\text{Acc}_{\text{obj}}\uparrow$	$\text{Acc}_{\text{tex}}\uparrow$	$\text{Acc}_{\text{shape}}\uparrow$	$\text{Acc}_{\text{all}}\uparrow$
Baseline	87.3	77.4	59.3	74.6
+ term1	91.3	84.7	65.6	80.5
+ term2	91.7	85.7	66.1	81.2

B.3. Evaluation of Cross-Attention Maps

We also provide the comparison of the cross-attention maps across various models, as illustrated in Fig. 5. In summary, our evaluation indicates that CosmicMan-SDXL exhibits enhanced precision in the generation of graphic t-shirt and black sneakers. This is further corroborated by our detailed examination of the attention maps for “Top Clothing”. Notably, the attention map corresponding to the “graphic” attribute demonstrates a more accurate activation in the top region, particularly when compared with the attention map extracted from SDXL. Furthermore, a comprehensive comparison of all attributes shows that CosmicMan-SDXL not only achieves higher semantic accuracy, but also achieves more accurate semantic activation in the corresponding attention map than the model fine-tuned on CosmicMan-HQ.

B.4. Evaluation of Optimization Strategies

In addition to appending a loss term through linearization and adjusting scalar coefficients, we conduct additional experiments employing a multi-objective optimization technique, Random Loss Weighting (RLW) [34], on CosmicMan-SD. The results presented in Tab. 9 reveal that both using RLW directly and combining it with a weighted loss term lead to a decline in model performance.

Table 9. **Ablation on Optimization Strategies.** The best results are marked with Red.

RLW	β	FID↓	$\text{Acc}_{\text{obj}}\uparrow$	$\text{Acc}_{\text{tex}}\uparrow$	$\text{Acc}_{\text{shape}}\uparrow$	$\text{Acc}_{\text{all}}\uparrow$
✓		55.5	83.7	76.7	60.8	73.6
✓	✓	39.9	89.9	81.7	63.2	78.2
	✓	36.8	91.7	85.7	66.1	81.2

C. Experiments

To more vividly demonstrate the performance of our text-to-image foundation model, CosmicMan, this section provides an extensive array of qualitative results. In Sec. C.1

and Sec. C.2, we begin by detailing our experimental procedures and evaluation metric. We then present the comparative qualitative results against the state-of-the-art models in Sec. C.3, followed by more visual results of the ablation studies in Sec. C.4. In Sec. C.5 and Sec. C.6, we provide further analysis on the visual results with different granularity, as well as different concepts, respectively. Sec. C.7 provides a fairness comparison on an unseen dataset. In Sec. C.8, we show the superiority of our foundation model over Stable Diffusion pretrained model on two downstream applications. Finally, we provide additional visualizations of our model in Sec. C.9.

C.1. Experiment Setting

Our foundation models CosmicMan contains two versions: CosmicMan-SD based on SD-1.5 [51], and CosmicMan-SDXL based on SDXL [45]. The DDPM Scheduler [22] and EulerAncestralDiscreteScheduler are used for training and testing, respectively. The HOLA loss only affects the cross-attention block at $16\times$ down-sampling rate. In CosmicMan-SDXL, the multi-aspect training strategy [45] in combination with an offset-noise level of 0.05 is utilized to train our foundation model, and the weight of HOLA loss is set to 1. In CosmicMan-SD, the weight of HOLA loss is set to 0.001 to avoid over-saturation problem. During the training process, a dropout strategy is applied with a probability of 0.1 to all attributes located in front of each object, as well as to the region description phrases, with the notable exception of the phrase “Overall”. Additionally, the photo type, derived from the keypoints, is systematically positioned at the forefront of the dense description. Besides, we also use the quality tuning technique [10] on both models to further enhance the final visually appealing. We finetune on 500 extremely high-quality human images with an offset-noise level of 0.05 for about 1000 iterations.

C.2. Fine-grained Text-Image Alignment Metric

We introduce **Semantic Acc**, a novel text-image alignment metric specifically designed for dense concepts in human images. Firstly, it adopts an atomized approach as other metrics for fine-grained text-image alignment [8, 23], breaking down descriptions into discrete questions to minimize coupling. This atomization is effectively implemented using a predefined question dictionary for finite human descriptions, thereby avoiding the additional errors introduced by generating questions through Large Language Models. For heightened precision, we fine-tuned a Vision-Language Model specifically to answer the atomized questions, rather than relying on pretrained models. Specifically, we ask “yes” or “no” questions for each atomic attribute using InstructBLIP. For example, for a generated image with input description of “plaid short sleeve t-shirt”, we would ask three questions sequentially: “Does the person wear a t-

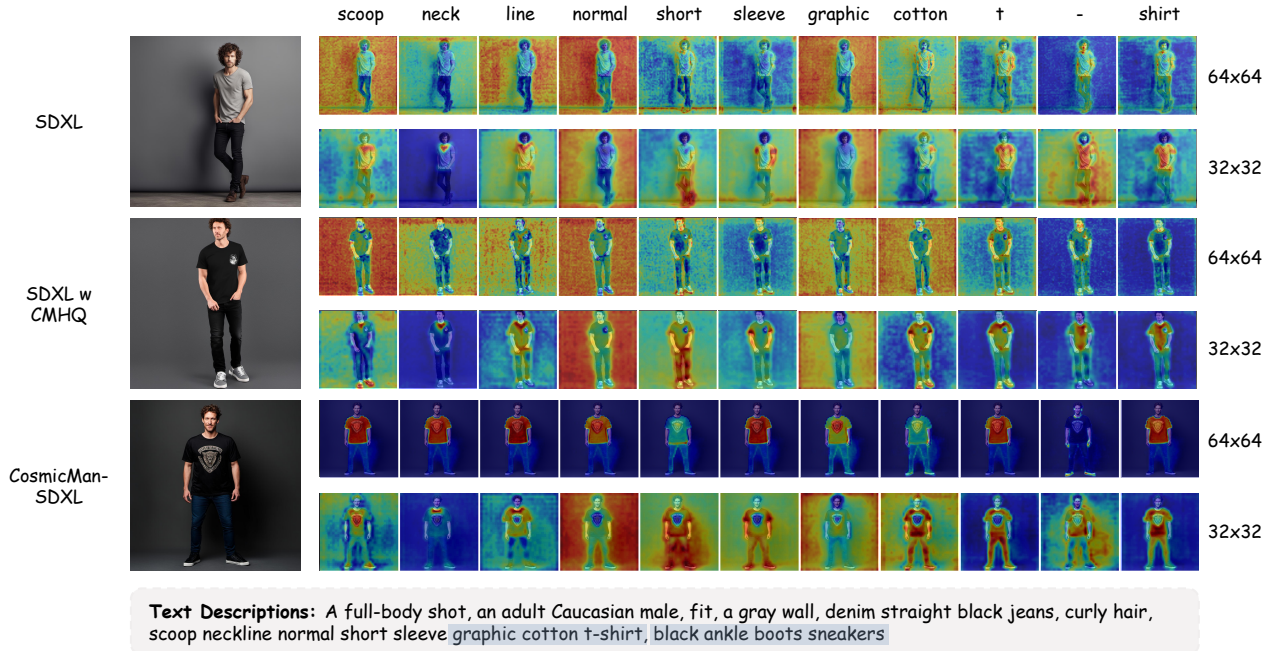


Figure 5. **Visualization of Cross-attention Maps.** We show cross-attention maps in SDXL-base for two different resolutions (map of 64×64 shape with $16 \times$ down-sampling and map of 32×32 shape with $32 \times$ down-sampling), in a similar way to the Prompt-to-Prompt [19] visualization method. For a clearer comparison, we further resize them to the original image size.

shirt?”, “Does the t-shirt have a plaid pattern?”, and “Is the t-shirt short sleeve?”. The answer to all three questions is “yes”. To prevent overfitting, attributes of the same hierarchy are randomly selected from CosmicMan-HQ 1.0 to generate “no” answer questions during training. The Semantic Acc scores are calculated by dividing the number of correct answers by the total number of questions. To further analyze text-image alignment for humans across various dimensions, we categorize Semantic Acc into three groups: Acc_{obj} for object types, Acc_{tex} for texture attributes, and $\text{Acc}_{\text{shape}}$ for shape attributes, as indexed in Tab. 6.

C.3. Qualitative Comparison to SOTA

We focus on comparing our two foundational models with state-of-the-art models such as SD-1.5, DALLE2, DALLE3, Midjourney, DeepFloyd-IF, and SDXL, as depicted in Fig. 6 and Fig. 7. While SD-1.5 shows the highest CLIPScore among these contenders, as highlighted in the main paper, its visual performance indicates subpar image quality and text-image alignment. Other models are able to generally produce human images that are consistent with detailed descriptions, though they sometimes omit or misinterpret certain concepts, which are highlighted by red dotted boxes in figures. For instance, in the first caption of Fig. 7, which depicts a white wedding dress and a black jacket, these models successfully generate the dress but fail to capture the concept of the black jacket. Re-

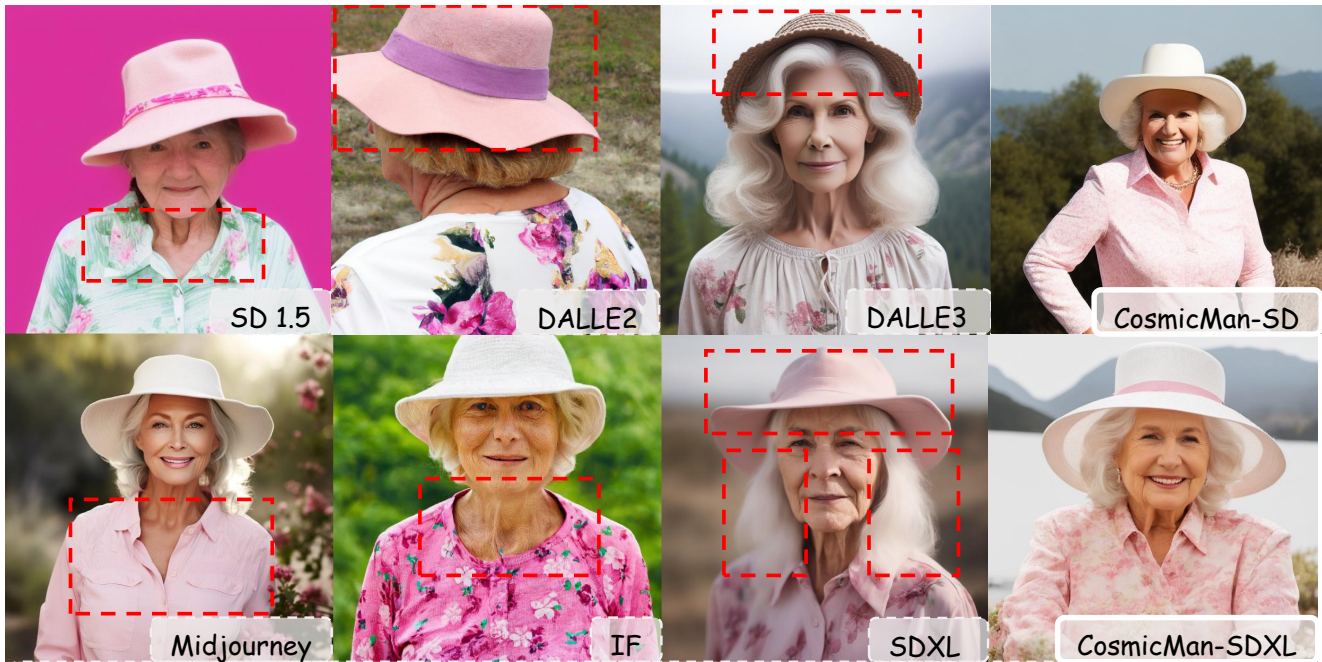
garding CosmicMan-SD, which possesses the same architecture as SD-1.5, it exhibits better text-image alignment. CosmicMan-SDXL excels in both image quality and text-image alignment for dense concepts.

C.4. Qualitative Ablation Studies

In this section, We provide qualitative results based on our setting to show the effectiveness of each part proposed in Daring.

Ablation on Training Dataset. In evaluating the efficacy of data sources, it is observed that the outputs derived from the model trained on CosmicMan-HQ 1.0 dataset exhibit a closer resemblance to authentic imagery and a higher text-image alignment when compared with those generated by models trained on LAION-5B and HumanSD. This comparative analysis is exemplified in Fig. 8, where the first row illustrates a notable discrepancy. The LAION-5B image is characterized by a slight overexposure, while the representation of clothing material in the HumanSD image deviates from a cotton-like texture.

Regarding the impact of data scaling on model performance, the training on the CosmicMan-HQ-6M dataset demonstrates enhanced precision in the text-image alignment for dense concepts. As evidenced in Fig. 8, the model trained with CosmicMan-HQ-6M more accurately captures fine-grained attributes, such as ankle boots (illustrated in the third row) and a striped skirt (depicted in the fourth row), in



Text Descriptions: An upper body shot, a Caucasian elderly female, natural landscape, white cotton hat, above shoulders wavy white hair, pink floral normal cotton long sleeve shirt

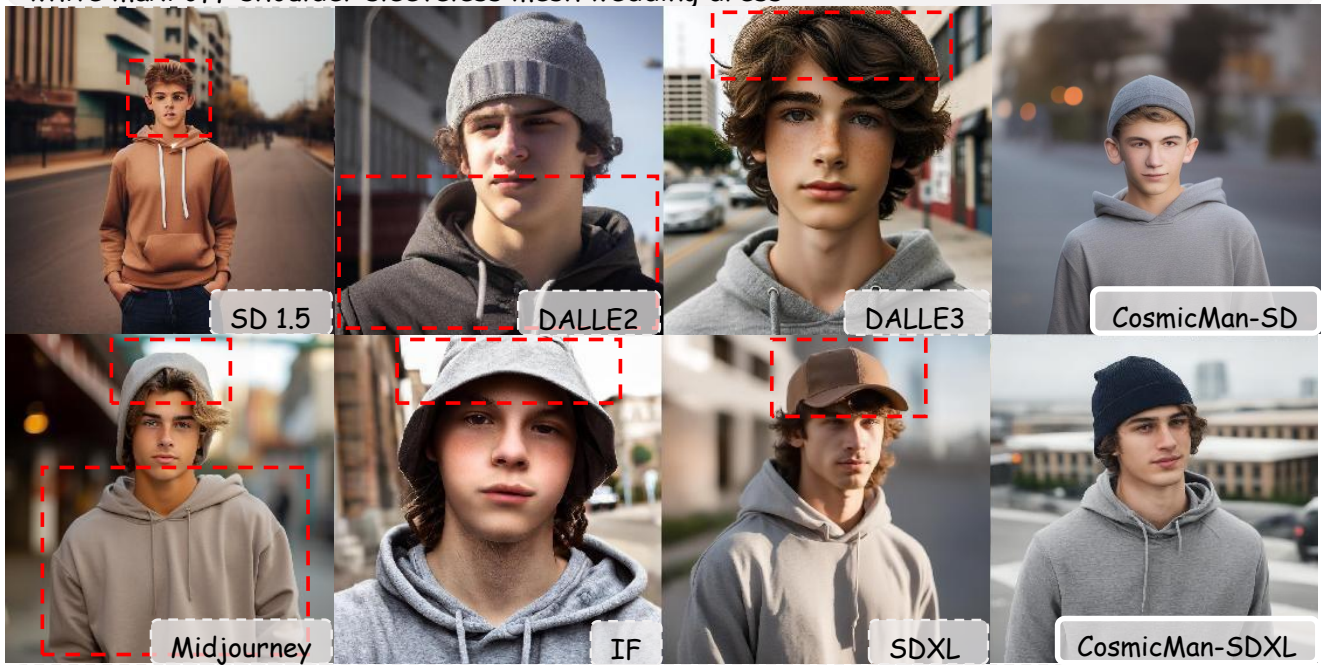


Text Descriptions: A full-body shot, an adult Caucasian female, fit, a white wall, brown straight hair, leather brown mid-calf boots, sleeveless off-shoulder midi silk graphic dress

Figure 6. **Comparison with State-of-the-art Models.** From left to right, the top row features the results of SD 1.5, DALLE2, DALLE3, and CosmicMan-SD. The bottom row presents the results of Midjourney 5.2, DeepFloyd-IF, SDXL, and CosmicMan-SDXL.



Text Descriptions: A nearly full-body shot, an adult Asian female, fit, a forest with trees and a sky with clouds, above eyes bun black hair, solid color cotton black jacket, solid color white maxi off-shoulder sleeveless mesh wedding dress



Text Descriptions: A close up portrait shot, a Caucasian teenager male, fit, a street with a building in the distance, cotton knitted hat, brown wavy above eyes hair, gray cotton long sleeve normal solid color hoodie

Figure 7. Comparison with State-of-the-art Models. From left to right, the top row features the results of SD 1.5, DALLE2, DALLE3 and CosmicMan-SD. The bottom row presents the results of Midjourney 5.2, DeepFloyd-IF, SDXL, and CosmicMan-SDXL.

LAION-5B

HumanSD-1M

CMHQ-1M-AltText

CMHQ-1M-IB

CMHQ-1M-AA

CMHQ-6M-AA



Text Descriptions: A close up portrait shot, an African adult male, fit, rooftop terrace overlooking a sprawling cityscape, crew cut bald black hair, **graphic** blue a jersey normal short sleeve cotton scoop neckline t-shirt, **plastic hat**



Text Descriptions: A close up portrait shot, a Caucasian child female, fit, blurred riverside, normal **graphic** cotton floral short sleeve **pink t-shirt**, close-fitting cotton solid color maxi **gray pants**, brown above shoulders bun hair



Text Descriptions: A full-body shot, an adult Caucasian female, fit, outdoor, solid color black leather **ankle boots high heels**, belt, cotton medium sleeve **plaid short dress**, above chest wavy blonde hair, leather clutch



Text Descriptions: A full-body shot, an Asian adult female, fit, a white wall, short white **stripes cotton skirt**, **solid color** short sleeve cotton **black crop off-shoulder top**, above chest wavy black hair

Figure 8. Ablation on Training Data. “AltText” refers to Web Alternative Text, “IB” denotes the image descriptions generated by the pretrained InstructBLIP model, “AA” corresponds to captions produced by Annotate Anyone, and “CMHQ” refers to the CosmicMan-HQ.

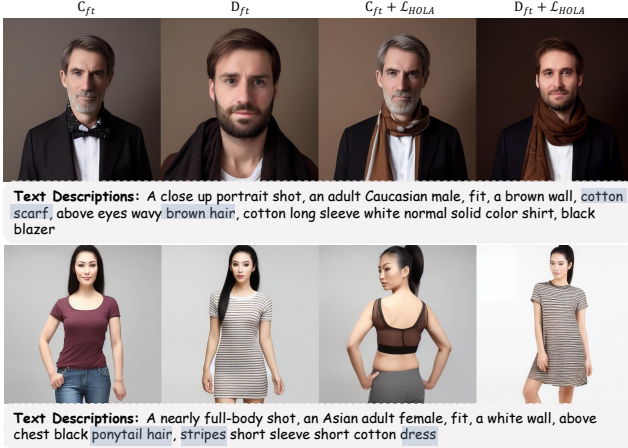


Figure 9. **Ablation on HOLA Loss and Data Discretization.** D_{ft} and C_{ft} denote fine-tuning and testing models on the continuous and decomposed text space. \mathcal{L}_{HOLA} represents the human body and outfit-guided loss for alignment. The blue backgrounds are utilized to accentuate the content of the generated pairs. This approach is consistently applied throughout the following images to maintain uniformity and enhance visual clarity.

contrast to its CosmicMan-HQ-1M counterpart.

Furthermore, the superiority of annotation quality in the Annotate Anyone becomes evident when contrasted with the pretrained IB model. This is particularly noticeable in the generation of more accurate and refined annotations, leading to significant improvements in the visual representation of items such as a graphic pink t-shirt and gray pants, as showcased in the second row of Fig. 8.

Ablation on Training Strategy. We delineate the impact of Data Discretization for Humans and the incorporation of HOLA loss on the accuracy of the generated images. Fig. 9 elucidates this effect by contrasting results obtained under decomposed and continuous text spaces, underscoring the significance of Data Discretization for Humans. The model D_{ft} demonstrates a heightened ability to accurately generate images of a cotton scarf (as depicted in the first row) and a striped dress (shown in the second row), compared to its counterpart, C_{ft} . This observation underscores the premise that a discrete text space is more adept at handling complex, dense concepts in our dataset. Nevertheless, the absence of constraints on key K in the attention block occasionally leads to instances of attribute misalignment. In an effort to address this, the integration of HOLA loss with Data Discretization for Humans is explored. This combination, represented as $D_{ft} + \mathcal{L}_{HOLA}$, culminates in a further enhancement of semantic alignment. The resulting images depict a more realistic representation of a cotton scarf and accurately colored hair in the first row, and a more precisely rendered striped dress and ponytail hair in the second row.

In an effort to further dissect the influence of HOLA loss,

a comparative analysis focusing on the individual contributions of each term within the loss function is conducted. This is depicted in Fig. 10, where the differential impacts of these terms are illustrated. Specifically, Term 1 is observed to facilitate the improved generation of attributes that are characteristic of larger regions. Examples of this can be seen in the enhanced depiction of a blue shirt and a black skirt on the left and right images, respectively. However, it is noted that Term 1 is less effective in accurately rendering attributes that are localized. For instance, the polo shirt on the left side is more akin to a t-shirt in its representation. This discrepancy can be attributed to the nuanced differences, such as the localized collar shape, which distinguishes a polo shirt from a t-shirt. By composing Term 2, the model exhibits a heightened proficiency in generating attributes pertinent to localized regions. This is evident in the more accurate portrayal of the cat pattern and the polo shirt on the left, as well as the distinct pattern of the t-shirt on the right.

C.5. Qualitative Results of Different Granularity

To illustrate CosmicMan’s ability in processing descriptions of varying granularity, we offer a visualization in Fig. 11 that features captions with progressively increasing detail. Initially, we start with a simple caption specifying different outfit types to generate the base human image. Subsequently, we incrementally enrich the description by adding details about texture, shape, and color. The step-by-step result reveals our model’s capability to produce high-quality human images that remain faithfully aligned with increasingly complex and dense concepts.

C.6. Qualitative Results of Different Concepts

We demonstrate the versatility of CosmicMan-SDXL in handling varying fine-grained descriptions, as depicted in Fig. 12. We only modify certain elements of the descriptions while keeping other components consistent. In the first row, we alter the descriptions of outfit shape, such as the sleeve length in the target region, resulting in visible changes, yet the overall spatial layout is maintained. Next, we explore different textures and colors, like fur floral dress, showcasing the model’s ability to incorporate unique dense concepts. Lastly, when modifying the outfit type, significant changes are observed in the human structure and scene layout.

C.7. Quantitative Comparison on Unseen Testset

We follow the experimental settings and provide an additional zero-shot evaluation on an unseen human subset, which contains 2048 images filtered from the MS-COCO 2014 validation subset [35]. As shown in Tab. 10, our models outperform all other methods in terms of image quality (FID). Regarding text-image alignment, we compare



Figure 10. **Ablation on Terms of HOLA Loss.** Baseline means only fine-tuning the model on CosmicMan-HQ 1.0. Term 1 refers to the first term of HOLA loss, which works under the guidance of human body structure. Term 2 refers to the second term of HOLA loss, which helps reduce the ambiguities of outfit-level descriptions.



Figure 11. **Qualitative Results of CosmicMan-SDXL with Increasing Granularity.** A simple description is initially provided, from which the granularity is progressively increased, emphasizing texture, shape, and color, leading to the generation of the following human images.

CLIPScore instead of Semantic Acc since the captions are in free-form text format. Its results consistently align with those from our original test set.

Table 10. **Quantitative Comparison on Unseen Human Testset.** We conduct zero-shot evaluation on MS-COCO 2014 validation subset. “CM-SD” and “CM-SDXL” are short for CosmicMan-SD and CosmicMan-SDXL.

Metrics	SD 1.5	SD 2.0	SDXL	DF-IF	CM-SD	CM-SDXL
FID	50.45	75.71	50.16	53.38	49.34	45.90
CLIP	27.23	23.58	27.37	26.96	27.23	25.56
Speed (ms/f)	43.66	55.99	56.23	203.43	43.53	56.32

C.8. Applications

In this subsection, we provide more qualitative results on two downstream applications: 2D human editing and 3D human reconstruction to show the effectiveness of our spe-

cialized foundation model.

2D Human Editing. We compare our CosmicMan-SDXL with SDXL pretrained model using T2I-Adapter [41]. We use skeleton maps extracted by Openpose [4] as guidance to generate portraits with specified poses. The first and second rows in Fig. 13 show that our results exhibit more accurate pose control. Besides, SDXL tends to generate semantic inconsistency images with a hazy background, while our method generates more realistic and semantic-consistent images.

3D Human Reconstruction. We further compare our CosmicMan-SD with SD-1.5 pretrained model based Magic123 [47] for 3D human reconstruction. The first two examples in Fig. 14 show the ability on Image-to-3D, where both reference image and prompt are used as input. The first example shows that our model can maintain the hat shape of the girl in each view, demonstrating that our model possesses better multi-view consistency. The second example

shows Stable Diffusion pretrained model tends to generate results with vague and odd human shapes (the 3rd and 6th images of SD in second example). In contrast, our results obtain more accurate human body and face geometric shapes. The third example in Fig. 14 shows the ability on Text-to-3D, where the single prompt is initially input to CosmicMan-SD or Stable Diffusion pretrained model to generate the reference image, and then sent to Magic123. It can be seen that our results are significantly superior to Stable Diffusion results on both text-image consistency and geometric shape.

C.9. More Generated Samples of CosmicMan

In Fig. 15 ~ Fig. 20, we present additional generated samples showcasing a variety of captions and aspect ratios. Please note that some images have been cropped for improved typesetting.



Figure 12. Qualitative Results of CosmicMan-SDXL with Different Descriptions on Shape, Texture, and Outfit Types.

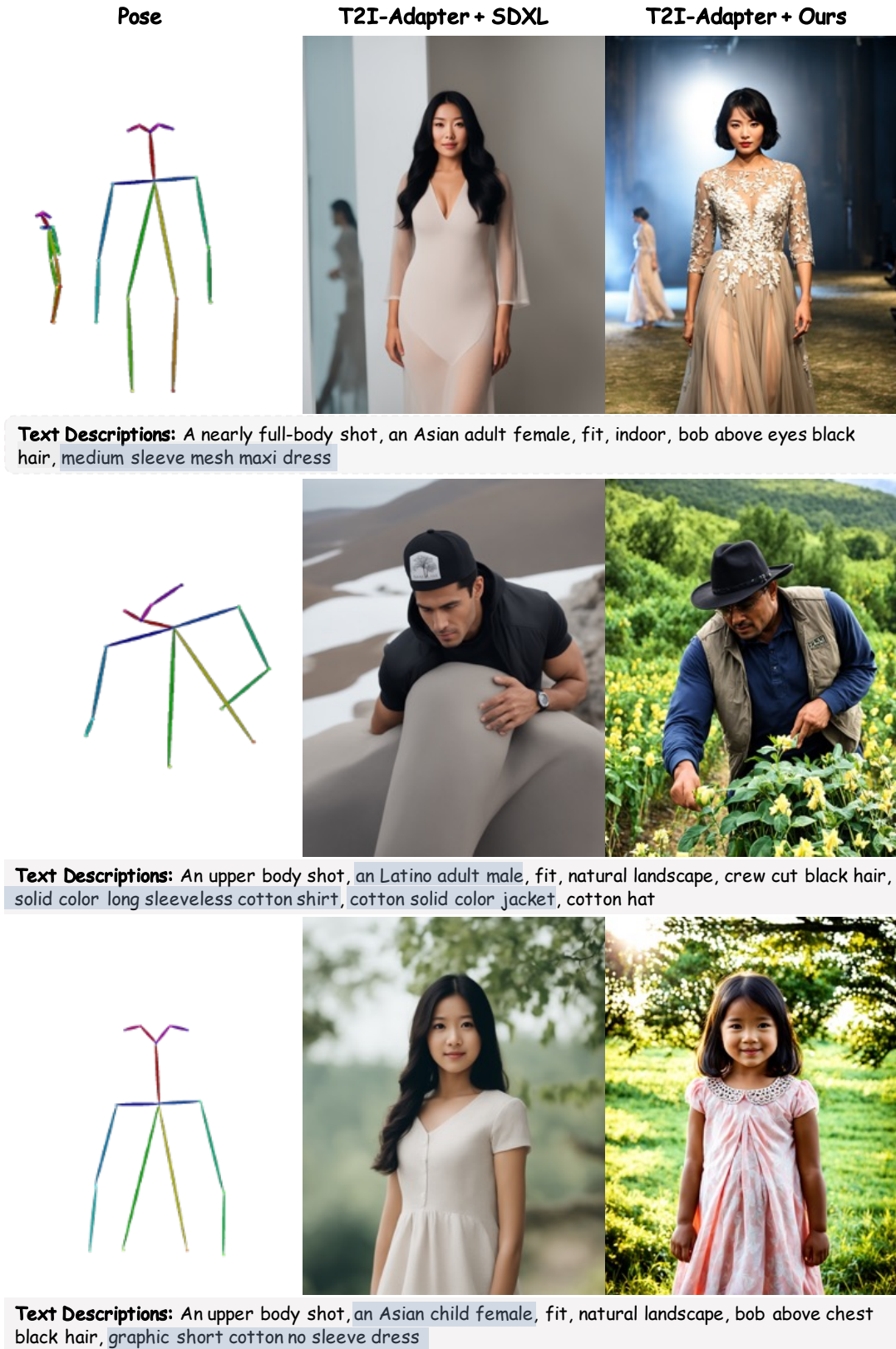
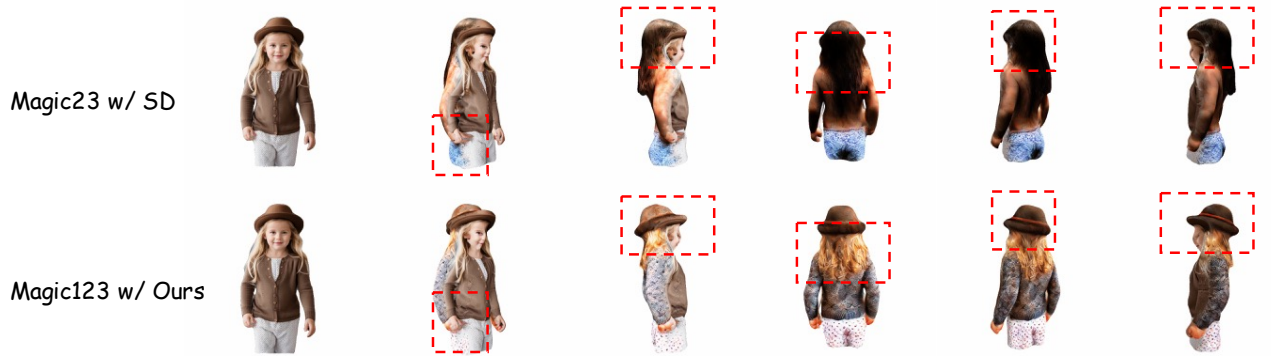
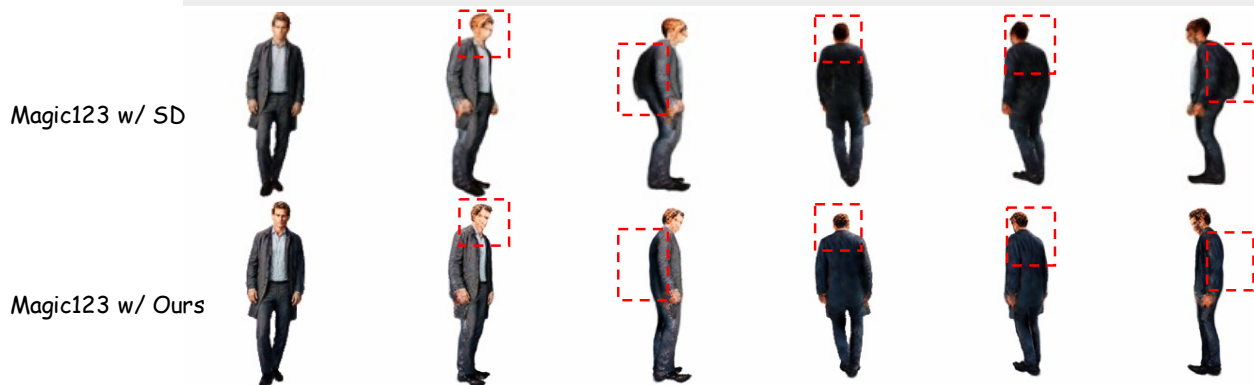


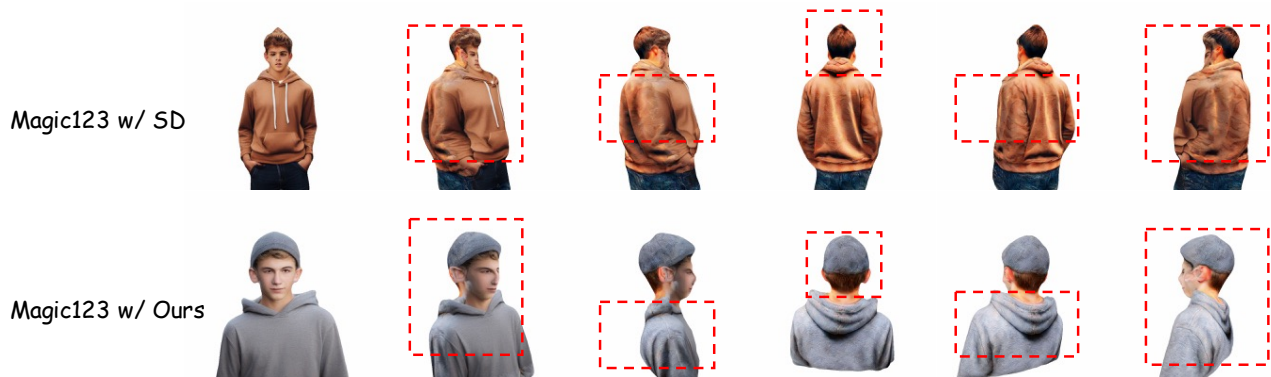
Figure 13. **Visualization of 2D Human Editing.** We compare our CosmicMan-SDXL with SDXL pretrained model based on T2I-Adapter [41]. We highlight the areas of text-image inconsistency of SDXL results in “Text Descriptions” using blue background.



Text Descriptions: An upper body shot, a Caucasian female child, fit, above chest blonde wavy hair, woven hat, straight maxi cotton graphic white polka dots pants, solid color normal woven brown long sleeve sweaters



Text Descriptions: A full-body shot, an adult Caucasian male, fit, wavy gold above eyes hair, solid color cotton normal long sleeve shirt, cotton solid color overcoat, solid color cotton straight maxi pants, solid color shoes



Text Descriptions: A close up portrait shot, a Caucasian teenager male, fit, a street with a building in the distance, cotton knitted hat, brown wavy above eyes hair, gray cotton long sleeve normal solid color hoodie

Figure 14. **Visualization of 3D Human Reconstruction.** We compare our CosmicMan-SD with Stable Diffusion pretrained model based on Magic123 [47]. The first and second examples show the ability of Image-to-3D. The third example shows the ability of Text-to-3D. CosmicMan-SD can generate results with better multi-view consistency and geometric shapes. The first image in each row is the reference image. Note that the reference images in the fifth and sixth are generated by CosmicMan-SD and SD-1.5 respectively. The red box highlights the improvement of our foundation model compared to Stable Diffusion.



Text Descriptions:

A close up portrait shot, an adult Caucasian female, fit, runway, cotton long sleeve solid color white normal t-shirt, solid color fur scarf, wavy above chest brown hair.



Text Descriptions:

A headshot, an adult Latino male, fit, softly blurred city traffic at night, solid color maxi cotton dress, above eyes wavy brown hair, solid color long sleeve cotton normal red t-shirt, cotton baseball cap.

Figure 15. More Generated Samples of CosmicMan.



Text Descriptions:
A close up portrait shot, an Asian child female, fit, fuzzy urban park with blurred walkers, sleeveless white cotton solid color normal camisole, above shoulders black bob hair.



Text Descriptions:
A close up portrait shot, an African adult female, fit, autumn forest, warm earthy blur, printed cotton scarf, cotton long sleeve black normal solid color t-shirt, above shoulders afro-hair black hair.

Figure 16. More Generated Samples of CosmicMan.



Text Descriptions:
A headshot, an adult Caucasian female, misty forest with distant mountains, above eyes brown bob hair.



Text Descriptions:
A headshot, a Caucasian adult male, fit, outdoor, normal white solid color long sleeve cotton shirt, white bald hair, solid color black jacket.



Text Descriptions:
A headshot, an Asian adult female, fit, a mountainous landscape, solid color cotton long sleeve short dress, above chest brown straight hair, solid color gray cotton overcoat.

Figure 17. More Generated samples of CosmicMan.



Text Descriptions:
A headshot, an adult Caucasian female, fit, softly blurred city traffic at night, above chest brown straight hair, gray cotton normal long sleeve solid color sweaters.



Text Descriptions:
A close up portrait shot, an adult Caucasian male, vaguely visible park with autumn trees, above eyes wavy brown hair, cotton long sleeve white normal solid color shirt.



Text Descriptions:
A close up portrait shot, an adult Caucasian female, fit, blurred riverside with distant boats, wavy red above chest hair, blue silk long sleeve normal blouse, silk midi long sleeve dress.

Figure 18. More Generated Samples of CosmicMan.



Text Descriptions:
A headshot, an adult Caucasian female, black and white city in distance, above chest blonde wavy hair.



Text Descriptions:
A headshot, a Caucasian elderly male, a blue wall, bald above eyes gray hair, blue short sleeve polo shirt, blue hat.



Text Descriptions:
A full-body shot, a Caucasian adult female, fit, outdoor, sleeveless solid color silk short off-shoulder jumpsuit, black bun above shoulders hair, leather solid color high heels



Text Descriptions:
An upper body shot, an adult Asian female, fit, dusk cityscape in dreamy blur, grey tie-dye long sleeve graphic cotton normal sweatshirt, tie-dye cotton graphic tapered grey maxi sweatpants, wavy above chest brown hair.



Text Descriptions:
An upper body shot, a Caucasian elderly female, fit, in a city traffic scene, white cotton hat, above shoulders wavy white hair, pink floral normal cotton long sleeve shirt.

Figure 19. More Generated Samples of CosmicMan.



Text Descriptions:
 A close up portrait shot, a Caucasian child female, fit, a white wall, normal graphic cotton floral short sleeve gray t-shirt, pink solid color leather sneakers, close-fitting cotton solid color maxi pink pants, brown above shoulders bun hair



Text Descriptions:
 A close up portrait shot, a Caucasian toddler male, fit, outdoor, blonde straight above eyes hair, long sleeve normal blue solid color cotton t-shirt.



Text Descriptions:
 A full-body shot, a Caucasian adult female, fit, outdoor, sleeveless solid color silk short jumpsuit, black bun above shoulders hair, solid color pink high heels.



Text Descriptions:
 A headshot, a Caucasian adult male, fit, summer forest, cold earthy blur, normal black solid color long sleeve cotton shirt, white bald hair, black ankle boots leather solid color loafers.



Text Descriptions:
 An upper body shot, a Caucasian adult female, fit, blurred riverside, fur solid color scarf, blonde wavy above shoulders hair, gray normal silk long sleeve solid color blouse, white solid color maxi straight cotton pants.



Text Descriptions:
 A close up portrait shot, an adult Caucasian female, fit, indoor, short sleeve solid color orange silk dress, leather belt, above shoulders wavy blonde hair.

Figure 20. More Generated Samples of CosmicMan.